Effects of spatially heterogeneous lakeside development on nearshore biotic communities in a large, deep, oligotrophic lake (Lake Baikal, Siberia)

Michael F. Meyer[1]*
Stephanie E. Hampton[2]
Ted Ozersky[3]
Kara H. Woo[2]
Kirill Shchapov[3]
Daniel D. Snow[4]
Emma J. Rosi[5]
Maxim A. Timofeyev[6]
Yulia M. Zaitseva[7]
Dmitry Yu. Karnaukhov[6]
Nina A. Bondarenko[7]
Aaron W. E. Galloway[8]
Julie Schram[8]
Matthew R. Brousil[2]

[1.] School of the Environment, Washington State University, Pullman, WA, USA
[2.] Center for Environmental Research, Education, and Outreach, Washington State University, Pullman, WA, USA
[3.] Large Lakes Observatory, University of Minnesota - Duluth, Duluth, MN, USA
[4.] School of Natural Resources, University of Nebraska-Lincoln, Lincoln, NE, USA
[5.] Cary Institute of Ecosystem Studies, Millbrook, NY, USA
[6.] Biological Research Institute, Irkutsk State University, Irkutsk, Irkutsk Oblast, Russia
[7.] Limnological Institute SB RAS, Irkutsk, Irkutsk Oblast, Russia
[8.] Oregon Institute of Marine Biology, University of Oregon, Charleston, OR, USA

*corresponding author: michael.f.meyer@wsu.edu

Keywords: sewage, PPCP, food webs, fatty acids, human disturbance

Abstract (248/250 words)

Sewage released from lakeside development can reshape ecological communities. In particular, nearshore periphyton can rapidly assimilate sewage-associated nutrients and increase filamentous algal abundance, thus altering both food abundance and quality for grazers. In Lake Baikal, a voluminous, ultra-oligotrophic, remote lake in Siberia, filamentous algal abundance has increased near lakeside developments, and localized sewage is the suspected cause. These shifts are of particular interest in Lake Baikal, where endemic littoral biodiversity is high, lakeside settlements are small (80 - 1,963 residents), tourism is high (~1.2 million visitors annually), and settlements are separated by large tracts of undisturbed shoreline, enabling investigation of heterogeneity and gradients of disturbance. We surveyed sites along 40 km of Baikal's southwestern shore for robust sewage indicators – pharmaceuticals and personal care products (PPCPs) and microplastics – as well as periphyton and macroinvertebrate abundance and indicators of food web structure (stable isotopes and fatty acids). PPCPs, including caffeine and acetaminophen/paracetamol, were spatially related to lakeside development. As predicted, lakeside development was associated with more filamentous algae and lower abundance of sewage-sensitive molluscs. Periphyton and macroinvertebrate stable isotopes and essential fatty acids suggested that food web structure otherwise remained similar across sites; yet, the invariance of amphipod fatty acid composition, relative to periphyton, suggested that grazers adjust behavior or metabolism to compensate for different periphyton assemblages. Our results demonstrate that even low levels of human disturbance can result in spatial heterogeneity of nearshore ecological responses, with potential for creating less visible effects that propagate through the food web.

Introduction

The release of treated and untreated wastewater into aquatic ecosystems is a common human disturbance that can introduce pollutants and reshape aquatic ecological communities (Hampton et al. 2011). Nitrogen and phosphorus are among the primary pollutants in wastewater and its associated byproducts (Smith et al. 1999), yet they can also originate from disparate anthropogenic and natural environmental sources, thereby complicating their use as sewage indicators. For example, agricultural runoff (Powers et al. 2016), watershed processes such as melting permafrost (Turetsky et al. 2000), and changes in terrestrial plant communities (Moran et al. 2012) can all increase allochthonous nutrient inputs similar to sewage. Regardless of the nutrients' source, biological processes can further confound sewage detection. Benthic primary producers, especially those in oligotrophic systems, can assimilate nutrients quickly from the water column (e.g., hours), such that elevated nutrient concentrations may not be not observed (Hadwen and Bunn 2005).

Because nutrients come from numerous non-sewage sources, indicators consistently associated with human activity, such as enhanced $\delta^{15}N$ stable isotope signatures (Costanzo et al. 2001;

Camilleri and Ozersky 2019), pharmaceuticals and personal care products (PPCPs) (Rosi-Marshall and Royer 2012; Meyer et al. 2019) and microplastics (Barnes et al. 2009), have garnered increasing attention for their usefulness as sewage indicators. Stable isotopes, such as $\delta^{15}N$, have been frequently used to trace sewage pollution (Gartner et al. 2002), yet their potential to indicate sewage can be obfuscated by complex terrestrial (Craine et al. 2018) and aquatic (Guzzo et al. 2011) processes. PPCP studies from continental (Kolpin et al. 2002; Focazio et al. 2008; Yang et al. 2018) to colloidal pore (Yang et al. 2016) scales, have shown that PPCP concentrations tend to be greatest closer to their source. In addition to identifying areas and periods of sewage pollution, PPCPs have also demonstrated robustness in defining gradients of sewage pollution in river systems, with concentrations being directly proportional to population density and inversely proportional to distance from a densely populated area (Bendz et al. 2005). Similar to PPCPs, microplastics (plastic debris up to 5 mm in size) also have been used to detect sewage pollution (Li et al. 2018) along gradients of increasing human population density (Klein et al. 2015). Microplastics are typically resistant to degradation (Barnes et al. 2009), providing a signal over a longer time frame than many PPCPs and nutrients in sewage. As a result of each pollutant's consistent association with sewage, co-located $\delta^{15}N$, PPCP, and microplastic measurements can be used to infer the spatial extent and timing of sewage pollution in an ecosystem.

The effects of sewage pollution are frequently first seen in nearshore benthic communities where increased nutrients alter algal species composition, abundance, nutritional quality, as well as trophic structure. Increased filamentous algal abundance, for example, has been frequently observed in areas suspected of sewage pollution (Rosenberger et al. 2008; Hampton et al. 2011), likely due to benthic filamentous algae efficiently removing nutrients from the water column (Hadwen and Bunn 2005; Andersson and Brunberg 2006). With a changing resource base, grazing macroinvertebrate communities may likewise shift to include more detritivores or species capable of consuming filamentous algae (Rosenberger et al. 2008). In addition to some grazers' physical difficulty consuming filamentous algae (Mazzella and Russo 1989), there also may be changes in algal nutritional quality, as filamentous algae tend to contain a different mixture of essential fatty acids (EFAs) in comparison to diatoms (Kelly and Scheibling 2012), which dominate periphyton communities in unimpacted ecosystems. In particular, the EFAs 18:3ω3 and 18:4ω3 are commonly associated with green filamentous algae (Taipale et al. 2013), whereas 20:5ω3 is more associated with diatoms (Taipale et al. 2013). All EFAs are largely synthesized by primary producers, and each related group produces strongly differentiated multivariate EFA signatures (Taipale et al. 2013; Galloway and Winder 2015). Consumers, can acquire fatty acids by grazing (Dalsgaard et al. 2003) or upgrading fatty acids at their own energetic expense (Sargent and Falk-Petersen 1988; Dalsgaard et al. 2003) and often reflect the fatty acid signatures of their diets. Thus, comparing consumer and producer fatty acid compositions can be used to infer how grazing patterns may have changed in tandem with increasing sewage pollution.

To investigate lake littoral community and food web responses to sewage pollution, we surveyed 40 km of Lake Baikal's shoreline for indicators of sewage pollution and metrics of benthic community composition and structure. Located in Siberia, Lake Baikal is the oldest, most voluminous, and deepest freshwater lake in the world (Hampton et al. 2018), with the majority of Baikal's biodiversity occurring in the littoral zone (Kozhova and Izmest'eva 1998). While Lake Baikal's pelagic zone is generally ultra-oligotrophic (Yoshida et al. 2003; O'Donnell et al. 2017), nearshore areas abutting lakeside settlements have shown distinct signs of eutrophication (Timoshkin et al. 2016). Much of Lake Baikal's shoreline lacks human development and Baikal's watershed is largely roadless and unpopulated (Moore et al. 2009). Despite largely lacking human development, uncharacteristic filamentous algal blooms have been occurring throughout the lake since 2010 (Kravtsova et al. 2014; Timoshkin et al. 2016; Volkova et al. 2018). While increased *Ulothrix* spp. abundance historically occurs in late summer (Kozhov 1963; Kozhova and Izmest'eva 1998), recent observations of *Spirogyra* spp. abundance at unprecedented levels are thought to be associated with increased nearshore nutrient concentrations (Volkova et al. 2018; Ozersky et al. 2018). Inadequate wastewater management in lakeside settlements is likely the main driver of these nearshore algal blooms (Timoshkin et al. 2016, 2018), motivating further research that might identify the extent to which sewage is altering nearshore communities

Given the growing evidence that Baikal's nearshore periphyton communities are responding to sewage inputs, our goal was to understand how littoral benthic community composition and interactions may be changing near areas with sewage pollution. This overarching goal can be divided into three main objectives:

1. to identify areas of wastewater pollution using robust sewage indicators,
2. to assess the relationship between sewage indicators and littoral periphyton and macroinvertebrate community composition, and
3. to evaluate how food webs may restructure with increasing sewage pollution.

We hypothesized that (1) sewage indicators, such as PPCP concentrations, $\delta^{15}N$, and microplastic densities, would increase with increasing population density and proximity of lakeside development; (2) an increasing sewage signal would correlate with increased dominance of filamentous benthic algae; and (3) increasing filamentous algae abundance would result in changes in the abundance of different macroinvertebrate feeding guilds, reflected in community composition and dietary tracers such as carbon and nitrogen stable isotopes and fatty acids.

Methods

1. *Site description*

The vast majority of Lake Baikal's 2,100-km shoreline lacks lakeside development (Moore et al. 2009; Timoshkin et al. 2016). Our study focused on a 40-km section of Baikal's southwestern shoreline, which included three settlements of different size (Figure 1). From 19 through 23 August 2015, we sampled 14 littoral and 3 pelagic locations along our 40-km transect. Littoral locations were chosen to capture a range of sites with varying degrees of adjacent shoreline development – from "developed" (along the waterfront of human settlements) to "undeveloped" (no adjacent human settlements and complete forest cover; Figure 1; Figure 2; Table 1). Pelagic sites were located 2 to 5 km offshore from each of the developed sites in water depths of 900-1300 m (Figure 1; Table 1). Littoral sites were sampled at approximately the same depth (~1.25 m) at a distance of 8.9-20.75 m from shore (Table 1). At each site, air temperature was measured with a mercury thermometer, and photographs were taken of the substrate and the shoreline.

Three discrete lakeside settlements occurred along our 40-km transect. The largest, Listvyanka, is primarily a tourist town with approximately 1,963 permanent residents, although tourism can contribute significantly to the town's population with 1.2 million annual visitors (Interfax-Tourism 2018). The other two settlements are the villages Bolshie Koty and Bolshoe Goloustnoe, which have approximately 80 and 600 permanent residents, respectively. Bolshie Koty is home to two field research stations and several small tourist accommodations. Bolshoe Goloustnoe has several hotels and tourist camps (IrkutskStat, 2012). Although Bolshie Koty and Bolshoe Goloustnoe are built along small streams that empty into Baikal, there are no upstream developed sites, meaning that any observed sewage indicators in Baikal most likely originated either from Bolshie Koty or Bolshoe Goloustnoe.

Inverse distance weighted (IDW) population calculation

We recognized that sewage indicator concentrations at each sampling location may be related to a sampling location's spatial position relative to both the size and proximity of neighboring developed sites. Therefore, we created the inverse distance weighted (IDW) population metric to compress, into a single metric, information about human population size, density, and location along the shoreline as well as distance between developed sites and sampling locations. The IDW metric reflects the idea that sewage pollution should be positively related to increasing human density and inversely related with distance from densely populated areas (sensu Bendz et al., 2005). Additionally, Timoshkin et al. (2018) noted that sewage enters Baikal's nearshore largely through groundwater, implying that locations with more directly adjacent shoreline development should experience higher sewage concentrations in the lake. Acknowledging that nearshore PPCP concentrations were likely positively proportional to a developed location's shoreline length, we scaled a developed site's population density by its shoreline length. This scaling represents population density that directly interfaces with the lake, thereby capturing the idea that sewage-associated pollutants, such as PPCPs (Karnjanapiboonwong et al., 2010) and

nutrients (de Vries, 1972), contributed away from the shoreline can be removed via the soil matrix en route to the lake.

Our workflow for calculating IDW population required five steps. First, we traced polygons and shorelines from satellite imagery for each developed site in Google Earth. Second, polygon and line geometries were downloaded from Google Earth as a .kml file. Third, the .kml file was imported into the R statistical environment (R Core Team, 2019), where using the sf package (Pebesma, 2018) we calculated shoreline length, polygon area, and centroid location for each developed site. Fourth, we joined point locations of each sampling site with the spatial polygons to calculate the distance from each sampling location to each developed site's centroid. Fifth, we calculated IDW population for each sampling location, using formula (1).

$$(1)\quad Ij = \frac{\frac{P_{LI}}{A_{LI}} * L_{LI}}{D_{j,LI}} + \frac{\frac{P_{BK}}{A_{BK}} * L_{BK}}{D_{j,BK}} + \frac{\frac{P_{BGO}}{A_{BGO}} * L_{BGO}}{D_{j,BGO}}$$

where I is the IDW population at sampling location j, P is the population at each of the three developed sites Listvyanka (LI), Bolshie Koty (BK), Bolshoe Goloustnoe (BGO), A is the area of a developed site in km^2, L is the shoreline length at a developed site in km, and D is the distance from developed site j to each developed site's centroid in km. This formulation implies that all sampling locations are influenced by all three developed sites. Thus, the influence of an individual developed site on each sampling location is positively influenced by the numerical and spatial density of the population and its orientation toward the shoreline, and inversely proportional to a sampling location's distance from each of the three developed sites.

2. Water samples

At both pelagic and littoral sites, water samples were collected for nutrient, chlorophyll, microplastic, and pharmaceutical and personal care product (PPCP) analysis. Samples were collected by hand from 0.75 m depth for each littoral site and with a bucket from aboard the Irkutsk State University "Kozhov" research vessel for pelagic sites. Each water sample collection procedure is described below.

2a. Nutrients

Water samples for nutrient analyses were collected in 150 mL glass jars that had been washed with phosphate-free soap and rinsed three times with water from the sampling location. Samples were collected in duplicates and immediately frozen at -20°C until processing at the A.P.Vinogradov Institute of Geochemistry (Siberian Branch of the Russian Academy of Sciences, Irkutsk). Samples were not filtered prior to freezing, meaning that nitrogen and ammonium concentrations may potentially include intracellular nitrogen and overestimate nitrogenous forms in the water column.

For each water sample, nitrate, ammonium, and total phosphorus concentrations were measured. For ammonium (2016a) and nitrate (2017) concentrations, samples were analyzed with a spectrophotometer following the addition of Nessler's reagent and disulfuric acid respectively. Total phosphorus concentration was measured with a spectrophotometer following the addition of persulfate (2016b). Concentrations are reported in mg/L.

2b. Chlorophyll a

Water samples were collected in 1.5 L plastic bottles from a depth of approximately 0.75 m. Within 12 h of collection, three subsamples (up to 150 mL each) were filtered through 25-mm diameter, 0.2 µm pore size nitrocellulose filters. Filters were then placed in a 35 mm petri dish and frozen in the dark until processing.

Chlorophyll samples were processed in a manner similar to that of Parson (1963) and Lorenzen (1967). Nitrocellulose filters were ground in 90% acetone, in which chlorophyll extraction was allowed to proceed overnight. Samples were then centrifuged for 15-20 minutes. After centrifugation, absorbance of the chlorophyll extract was measured in a spectrophotometer at 630, 645, 665, and 750 nm. Concentrations were calculated using the formula: $C = 11.64(A_{665} - A_{750}) - 2.16(A_{645} - A_{750}) - 0.1(A_{630} - A_{750}) / (V_2/V_1)$; where A is the absorbance value of a particular wavelength, V_1 is the volume of the filtered water, and V_2 is the volume of extract. Concentrations are reported as mg/L.

2c. PPCPs

Water samples for PPCP analysis were collected in 250 mL amber glass bottles that were rinsed with either methanol or acetone and then three times with sample water prior to collections. Following collection, samples were refrigerated and kept in the dark until solid phase extraction (SPE).

Within 12 h of collection, samples were filtered directly from the amber glass bottle using a single-stream 25-mm GF/F SPE cartridge setup (Waters Corporation, Milford, MA). Lab personnel wore gloves and face masks to minimize contamination. Prior to filtration, SPE cartridges were primed with at least 5 mL of either methanol or acetone and then washed with at least 5 mL of sample water. Rate of SPE occurred at approximately 1 drop per second. Extraction proceeded until water could no longer pass through the SPE cartridge or until all collected water was filtered. Cartridges were stored in Whirlpacks at -20°C until analysis for PPCPs following methods of Lee et al. (2016). Concentrations are reported in ng/L.

2d. *Microplastics*

At each location, samples were collected in triplicate using 1.5 L clear plastic bottles that were washed thoroughly with sample water before each collection. Samples were collected by hand for each littoral site and with a metal bucket from aboard the ship for pelagic sites.

For processing, each sample was vacuum filtered on to a 47-mm diameter GF/F filter. During filtration, aluminum foil was used to cover the filtration funnel to prevent contamination from airborne microplastic particles. After filtration, filters were dried under vacuum pressure and then stored in 50-mm petri dishes. Following filtration of all three replicates, the filtrate was collected and then re-filtered through a GF/F filter as a control for contamination from the plastic vacuum funnel or potentially airborne microplastics.

Microplastic counting involved visual inspection of the entire GF/F according to Van Cauwenberghe et al. (2015). Visual enumeration was conducted under a stereo microscope with ~100x magnification, and microplastics were classified into one of three categories: fibers, fragments, or beads. For all categories, plastics were defined as observed objects with apparent artificial colors, so as to not enumerate plastics contributed from the sampling bottle itself. Fibers were defined as smooth, long plastics with consistent diameters. Fragments were defined as plastics with irregularly sharp or jagged edges. Beads were defined as spherical plastics. During enumeration, GF/Fs remained in the petri dish to minimize potential for contamination from the air. Following enumeration of both experimental and control samples, fibers, fragments, and beads enumerated in the controls were subtracted from the experimental microplastic densities for each plastic type and from each replicate. One location (BK-1) had two control replicates, which were averaged for each plastic type and then subtracted from the experimental samples. Results are reported as the average number of microplastics/L.

3. Benthic biological samples

At each littoral site, periphyton and macroinvertebrates were collected for relative abundance estimates and food web analysis by wading and snorkeling.

3a. Benthic algal collection

At each littoral site, we haphazardly selected three rocks representative of local substrate. A plastic stencil was used to define a surface area of each rock from which we scraped a standardized 14.5 cm^2 patch of periphyton. Samples were preserved with Lugol's solution and stored in plastic scintillation vials. Additional periphyton was collected in composite from each site for fatty acid and stable isotope analysis.

Periphyton taxonomic identification and enumeration was performed by subsampling 10 µL aliquots from each preserved sample. Cells, filaments, and colonies were counted for each

taxonomic group until at least 300 cells were identified. For all 10 µL aliquots, the entire subsample was counted, even if 300 cells were counted prior to completing the aliquot. Taxa were classified into broad categories consistent with Baikal algal taxonomy (Izhboldina, 2007), using coarse groupings to capture general patterns in relative algal abundance. As a result, algal groups consisted of diatoms, *Ulothrix*, *Spirogyra*, and the green algal Order Tetrasporales.

3b. Benthic invertebrate collection

At each littoral site, three kick-net samples were collected for assessment of benthic community composition and abundance. Using a D-net, we collected macroinvertebrates by flipping over 1-3 rocks, and then sweeping five times in a left-to-right motion across approximately 1 m. After the series of sweeps, the catch was rinsed into a plastic bucket. For each replicate, bucket contents were concentrated using a 64 µm mesh and placed in glass jars with 40% ethanol (vodka; the only preservative available to us at the time) for preservation and refrigerated at 4°C aboard the research vessel. The 40% ethanol preservative was replaced with ~80% ethanol upon return to the lab within 24 to 48 hours, and samples were stored at ~4°C.

Separate collections were conducted for invertebrate fatty acid and stable isotope analyses. Invertebrates were collected using a D-net in a similar fashion as the community enumeration. Additional invertebrates were also collected by hand. Collected organisms were then live-sorted, identified to species, and frozen at -20°C at the field station. The samples were later transferred to the lab in the US via a Dewar flask with dry ice.

Invertebrate taxonomic identification and enumeration were performed under a stereo microscope. All invertebrates were identified to species with the exception of juveniles (Taakhteev, 2015 for amphipods; Sitnikova, 2012 for molluscs; Table 2). All samples contained oligochaetes and polychaetes, but due to poor preservation, these taxa were not counted. Six samples of the 42 collected were not well-preserved and were excluded from further analyses, in order to reduce errors in identification. KD-1 and LI-1 were the only sites with 1 sample counted. BK-2 and KD-2 each had two samples counted.

3c. Food web characterization

To characterize littoral food webs, we analyzed carbon and nitrogen stables isotopes as well as fatty acid profiles for periphyton and macroinvertebrates. Prior to isotopic and fatty acid analysis, periphyton and macroinvertebrate samples were lyophilized for ~24 hours, homogenized to powder, and then weighed.

Stable isotope analysis

Measurements of $\delta^{15}N$ and $\delta^{13}C$ were performed on an elemental analyzer-isotope ratio mass spectrometer (EA-IRMS; Finnigan DELTAplus XP, Thermo Scientific) at the Large Lakes Observatory, University of Minnesota Duluth. The EA-IRMS was calibrated against certified reference materials including L-glutamic acid (NIST SRM 8574), low organic soil and sorghum flour (standards B-2153 and B-2159 from Elemental Micro-analysis Ltd., Okehampton, UK) and in-house standards (acetanilide and caffeine). Replicate analyses of external standards showed a mean standard deviation of 0.06 ‰ and 0.09 ‰, for $\delta^{13}C$ and $\delta^{15}N$, respectively.

Fatty acid analysis

Following freeze-drying, samples were transferred to 10 mL glass centrifuge vials, and 2 mL of 100% chloroform was added to each under nitrogen gas. Samples were allowed to sit in chloroform overnight at -80°C. Fatty acid extractions generally involved three phases: (1) 100% chloroform extraction, (2) chloroform-methanol extraction, and (3) fatty acid methylation. Fatty acid extraction methods were adapted from Schram et al. (2018).

After overnight chloroform extraction, samples underwent a chloroform-methanol extraction three times. To each sample, we added 1 mL cooled 100% methanol, 1 mL chloroform:methanol solution (2:1), and 0.8 mL 0.9% NaCl solution. Samples were inverted three times and sonicated on ice for 10 minutes. Next, samples were vortexed for 1 minute, and centrifuged for 5 minutes (3,000 rpm) at 4°C. Using a double pipette technique, the lower organic layer was removed and kept under nitrogen. After the third extraction, samples were evaporated under nitrogen flow, and resuspended in 1.5 mL chloroform and stored at -20°C overnight.

Once resuspended in chloroform, 1 mL of chloroform extract was transferred to a glass centrifuge tube with a glass syringe as well as an internal standard of 4 µL of 19-carbon fatty acid. Samples were then evaporated under nitrogen, and then 1 mL of toluene and 2 mL of 1% sulfuric acid-methanol was added. The vial was closed under nitrogen gas and then incubated in 50°C water bath for 16 hours. After incubation, samples were removed from the bath, allowed to reach room temperature and stored on ice. Next, we performed a potassium carbonate-hexane extraction twice. To each sample, we added 2 mL of 2% potassium bicarbonate and 5 mL of 100% hexane, inverting the capped vial so as to mix the solution. Samples were centrifuged for 3 minutes (1,500 rpm) at 4°C. The upper hexane layer was then removed and placed in a vial to evaporate under nitrogen flow. Once almost evaporated, 1 mL of 100% hexane was added and stored in a glass amber autosampler vial for GC/MS quantification. GC/MS quantification was performed with a Shimadzu QP2020 GC/MS following Schram et al. (2018).

4. Statistical analyses

Total phosphorus, nitrate, ammonium, microplastic abundance and density, total PPCP concentration, and $\delta^{15}N$ in macroinvertebrate tissues were log-transformed and regressed against

log-transformed IDW population using a linear model. Analytically, log-transforming made sites comparable, as values spanned three orders of magnitude. Physically, we assumed that sewage indicators were likely subject to exponential processes (e.g., mixing, diffusion), and log-transforming the data should linearize the relationships between predictor and response variables. Residuals were assessed for normality and homogeneity of variance.

To assess if benthic community composition was associated with increasing sewage indicators, periphyton and macroinvertebrate abundance data were each analyzed with a consistent multivariate workflow. First, replicates were averaged, and taxonomic groups representing less than 1% of the inter-site community were removed from analysis, in order to reduce the influence of rare species on results. Second, community compositions for both periphyton and macroinvertebrates were visualized using non-metric multidimensional scaling (NMDS) with a Bray-Curtis similarity metric. Periphyton community compositions were calculated as relative proportions, whereas invertebrate abundances were grouped at the genus-level and then square-root transformed to minimize influence of more abundant taxa. Visual inspection of the NMDS plot suggested that sites generally tended to separate by increasing PPCP concentrations and IDW population. To test whether sites benthic communities significantly differed with increasing PPCP concentration and IDW population, we first used both k-mediods, also known as Partitioning Around the Mediods (PAM; Kaufman and Rousseeuw 2005), clustering and to identify an optimal number of groupings (Figure S1), for which we iterated through multiple numbers of clusters (i.e., 1 to 10) and calculated the within-group-sum-of-squares (wss) and silhouette width. We identified the optimal number of groups when wss decreased most markedly and when silhouette width was greatest (e.g., the elbow method) (Johnson and Wichern 2007). To confirm optimal number as determined by PAM, we also used Weighted Pair-Group Centroid Clustering (WPGMC) as a hierarchical approach (Sneath and Sokal 1973), which corrects for clusters that may not be strongly discriminated regardless of how many samples are assigned to a given cluster (Legendre and Legendre 2012). We then performed two permutational multivariate analyses of variance (PERMANOVA; Anderson 2001) with 999 permutations: the first where community compositions were responses to the groups identified through clustering and the second where community compositions were responses to the continuous IDW population. Together, these two PERMANOVAs allowed us to demonstrate whether IDW population was indeed reflected in the IDW groupings. Unlike traditional multivariate analyses of variance (MANOVA), PERMANOVA does not require assumptions of multivariate normality (Anderson 2001). When significant differences were identified, post-hoc SIMPER analysis (Clarke 1993) was performed following the PERMANOVA to identify which taxonomic groups contributed to 85% of the cumulative variance that most influenced site separation.

To assess if benthic food webs restructured with increasing sewage indicator concentrations, fatty acid data were analyzed in a manner similar to periphyton and macroinvertebrate

abundance data. First, species' fatty acid profiles were visualized by performing NMDS with Bray-Curtis similarity for all organisms' relative fatty acid abundance (Figure S2). This technique broadly demonstrated that, as expected, interspecific variation in fatty acid composition was greater than intraspecific variation. The same pattern was observed for all fatty acids quantified as well as solely essential fatty acids (EFAs; Figure S2). Together, these NMDS plots suggested that periphyton fatty acids at sites differentiated based on sewage indicator concentrations, which was likely a reflection of differences in community composition (Taipale et al. 2013). Among all taxa and sites, 18:3ω3, 18:1ω9, and 20:5ω3 had the highest coefficients of variation, enabling comparisons between sites. These fatty acids tend to be associated with filamentous green algae (i.e., 18:3ω3 and 18:1ω9) and diatoms (i.e., 20:5ω3). To increase the robustness of our analysis, we expanded our approach to include major fatty acids within each taxonomic group, including 18:2ω6 (abundant in green algae); 16:1ω7 and 14:0 (abundant in diatoms); and 16:0 (abundant in both green algae and diatoms) (Taipale et al. 2013). To evaluate how relative fatty acid abundance may relate to sewage pollution, we assessed patterns among these seven fatty acids both in multivariate and in univariate space. With a multivariate framework, we created two NMDS plots with Bray-Curtis similarity, one just with primary producer (Figure S5) and the other with macroinvertebrate (Figure S6) fatty acid profiles. Because multivariate patterns suggested fatty acid profiles may relate to sewage pollution, we regressed a filamentous:diatom fatty acid signal ratio (Equation 2)

$$(2)\ \frac{18{:}3\omega3\% + 18{:}1\omega9\% + 18{:}2\omega6\% + 16{:}0\%}{20{:}5\omega3\% + 16{:}1\omega7\% + 16{:}0\% + 14{:}0\%}$$

against log-transformed PPCP concentrations using a linear model. Additionally, we evaluated how three essential fatty acids (18:3ω3, 18:2ω6, and 20:5ω3), lipids thought to accumulate in biological systems, may differ in abundance across the sewage gradient. Therefore, we similarly regressed the ratio of $\frac{18{:}3\omega3\% + 18{:}2\omega6\%}{20{:}5\omega3\%}$ against log-transformed PPCP concentrations using a linear model.

All analyses were conducted in the R statistical environment (R Core Team 2019), using the tidyr (Wickham and Henry 2019), dplyr (Wickham et al. 2019), ggplot2 (Wickham 2016), and vegan (Oksanen et al. 2019) packages. All data, including .kml files used to calculate IDW metric, are publicly available from the Environmental Data Initiative repository (DOI), and all R scripts are available from the GitHub repository of this project's Open Science Framework account (DOI).

Results

1. Water samples

Nitrate ($R^2 = 0.01$, $p = 0.62$), ammonium ($R^2 = 0.12$, $p = 0.15$), and chlorophyll a ($R^2 = 0.20$, $p = 0.11$) were not significantly correlated with IDW population (Figure 3). Total phosphorus ($R^2 = 0.19$, $p = 0.08$) approached significance, and total PPCP ($R^2 = 0.30$, $p = 0.02$) concentrations

were significantly related with IDW population (Figure 3). Within the littoral zone, PPCPs detected included caffeine, 1,7-dimethylxanthine (main human metabolite of caffeine), cotinine (main human metabolite of nicotine), and acetaminophen (Table 3).

Microplastics were detected in samples from both the littoral and pelagic sites. Bead microplastics were only detected near Listvyanka. Fibers (mean = 0.85 microplastics/L, std dev = 1.21 microplastics/L) and fragments (mean = 0.83 microplastics/L, std dev = 1.35 microplastics/L) were the most abundant types of microplastics across all sites, whereas beads were relatively rare (mean = 0.08 microplastics/L, std dev = 0.31 microplastics/L). Total microplastic densities were not significantly correlated with IDW population ($R^2 = 0.03$, $p = 0.53$; Figure 3), although more types of microplastics were generally observed near areas with higher IDW population values, such as Listvyanka.

2. Benthic biological samples

2a. Periphyton

Major taxonomic groupings of periphyton consisted of diatoms, *Tetrasporales* spp., *Spirogyra* spp., and *Ulothrix* spp. K-mediods (Figures S1a; S2a) cluster and WPGMC (Figure S3a) analyses of periphyton abundance demonstrated two groupings capture most variance, and visual inspection of relative periphyton community abundance NMDS suggested groupings were related to IDW population values (Figure 4). PERMANOVA results demonstrated that periphyton communities were significantly different based on IDW population groupings ($R^2 = 0.40$, $p = 0.001$) and the continuous IDW population ($R^2 = 0.52$, $p = 0.001$). Post-hoc SIMPER results suggested that these differences were primarily associated with sites that had higher *Ulothrix* spp. relative abundance. Additionally, sites with high IDW populations had higher diatom relative abundance in comparison to sites with low IDW populations, yet not for sites with moderate IDW populations.

2b. Macroinvertebrates

Taxonomic groupings included five amphipod genera: *Eulimnogammarus*, *Poekilogammarus*, *Cryptoropus*, *Brandtia and Pallasea*; six mollusc families: Planorbidae, Valvatidae, Baicaliidae, Benedictidae, Acroloxidae, Maackia; flatworms; caddisflies; and leeches (summarized in Table S1). K-means cluster analysis of macroinvertebrate community composition suggested 2 or 3 major groupings would capture most variance (Figure S1b; S2b), whereas WPGMC analyses suggested 2 groupings would enable all sites except for one to be assigned a cluster (S3b). Because both forms of hierarchical and non-hierarchical clustering suggested two groupings as optimal, we proceeded using two groupings. Visual inspection of NMDS suggested clusters were related to IDW population (Figure 4). PERMANOVA results supported the hypothesis that

514 macroinvertebrate communities significantly differed both among our IDW population groupings
515 (R^2 = 0.19, p = 0.02) and along our continuous gradient of increasing IDW population (R^2 =
516 0.19, p = 0.02). Post-hoc SIMPER analyses suggested that *Poekilogammarus*,
517 *Eulimnogammarus*, *Valvatidae*, Caddisflies, *Brandtia*, *Baicaliidae*, and *Planorbidae* contributed
518 the greatest differences between high and moderate/low IDW population groupings.
519
520 *3. Food web characterization: stable isotopes and fatty acids*
521
522 Among periphyton and amphipod samples, $\delta^{13}C$ values ranged from -19.5 to -9.5 ‰ (Figure 5).
523 Among periphyton samples, $\delta^{15}N$ values ranged from 0.77 to 3.76 ‰, whereas amphipod $\delta^{15}N$
524 values ranged from 6.42 to 7.92 ‰.
525
526 For grazers, $\delta^{15}N$ significantly increased with IDW population (p = 0.008; Figure 3, Figure 5).
527 Periphyton $\delta^{15}N$ signatures did not significantly increase with IDW population (p = 0.7). In
528 contrast, $\delta^{13}C$ concentrations were not related with IDW population for either periphyton or
529 macroinvertebrates.
530
531 With respect to fatty acids, macroinvertebrates tended to be characterized by mono-unsaturated
532 fatty acids (MUFAs) and long-chain (i.e. ≥ 20-Carbons) polyunsaturated fatty acids (LCPUFAs),
533 whereas periphyton tended to be characterized by short-chain (i.e., 16- and 18-Carbons)
534 polyunsaturated fatty acids (SCPUFAs) (Table 3). When comparing proportions within taxa
535 across the sewage gradient, periphyton SCPUFA proportion tended to increase (Figure S4) and
536 periphyton SAFA proportions generally decreased. In contrast, benthic macroinvertebrate fatty
537 acid class proportions tended to remain consistent across the entire gradient (Figure S4).
538
539 For both periphyton and grazers, our analyses focused mainly on the fatty acids consistently
540 associated with filamentous green algae (i.e., 18:3ω3, 18:1ω9, 18:2ω6, and 16:0) as well as
541 diatoms (i.e., 20:5ω3, 16:1ω7, 14:0, and 16:0). For periphyton, the ratio of green
542 filamentous:diatom-associated fatty acids significantly increased with an increasing PPCP
543 concentration (R^2 = 0.62; p = 0.04, Figure 6; S5) but not with an increasing IDW population (p =
544 0.17). Amphipod fatty acid ratios were not significantly related with either increasing IDW
545 population or increasing PPCP concentrations (Figure 6; S6). When focusing solely on the
546 essential fatty acids 18:3ω3, 18:1ω9, and 20:5ω3, the same pattern was observed in both
547 periphyton (R^2 = 0.73; p = 0.02) and amphipods (Figure 6).
548
549 **Discussion**
550
551 Our combined results corroborate previous findings (e.g., Timoshkin et al., 2016; 2018) that
552 sewage pollution is entering Lake Baikal's nearshore area and likely is responsible for changes in
553 nearshore benthic communities. Unlike previous studies, we incorporate highly specific

554 indicators of sewage pollution and food web structure to offer direct, quantitative relationships
555 between human development and ecological responses.
556
557 *Relating human settlements to sewage indicator concentrations*
558
559 In agreement with our expectations, some sewage pollution indicators in the nearshore of Lake
560 Baikal were associated with size of and distance from human settlements. Total PPCP,
561 macroinvertebrate $\delta^{15}N$, and, to some degree, total phosphorus concentrations increased with
562 IDW population. These sewage gradients created by highly localized settlements are noteworthy
563 considering that Baikal's shoreline, including our study area, is largely free of lakeside
564 development (Moore et al. 2009). Furthermore, the use of sewage-associated indicators, such as
565 PPCPs and $\delta^{15}N$, proved necessary for defining sewage gradients. The use of nutrients as
566 indicators alone would not reveal sewage pollution gradients, since nutrients were not strongly
567 correlated with IDW population and could come from diverse sources. For example, melting
568 permafrost in Lake Baikal's watershed (Anisimov & Reneva, 2006) and the Selenga River basin
569 (Tornqvist et al., 2014) have the potential to contribute substantial nutrient loadings. While
570 nutrients also could be contributed by agriculture (Powers et al., 2016), atmospheric deposition
571 (Galloway et al. 2004; Monteith et al. 2007; Stoddard et al. 2016), and changing terrestrial plant
572 communities (Moran et al., 2012), these are not currently known to be major sources of elevated
573 nutrients in the Baikal watershed, relative to sewage (Timoshkin et al., 2016, Timoshkin et al.,
574 2018) and permafrost melt (Anisimov & Reneva, 2006).
575
576 This is the first study to detect PPCPs in Lake Baikal, a voluminous lake in a largely unpopulated
577 watershed. We detected PPCPs nearshore but not at our three offshore sites, suggesting that
578 sewage inputs in Baikal may dilute as pollutants diffuse out of the nearshore area. More
579 generally, these results are important for lake monitoring, as PPCPs are robust indicators of
580 sewage pollution. Beyond Lake Baikal, these data are important for understanding PPCPs'
581 prevalence in lakes, as lakes have remained less represented in the PPCP literature in comparison
582 to lotic and subsurface systems (Meyer et al. 2019). This literature imbalance creates opportunity
583 to assess how PPCPs, and sewage pollution more broadly, may lead to differing ecological
584 responses in lotic and lentic systems. As lakes tend to have longer hydraulic residence times
585 relative to rivers and streams, pollutants may be more prone to accumulate (Yang et al. 2018;
586 Meyer et al. 2019). In the case of our data, comparing contemporaneous littoral and pelagic
587 PPCP concentrations revealed new gradients, as PPCPs were degraded, metabolized or
588 accumulated by biota, or diffused to undetectable concentrations. In the context of the entire
589 lake, analyses of sediments have shown how PPCPs can remain within lake systems for decades,
590 thereby enabling researchers to reconstruct histories of wastewater pollution in a system
591 (Czekalski et al. 2015; Yang et al. 2018).
592

Investigating PPCP concentrations across limnic environments could also establish how ecological communities respond differently not only to sewage but also to the PPCPs themselves. While we focus on PPCPs as indicators of sewage, previous studies have shown that PPCPs, even at concentrations we observed in Lake Baikal, can elicit biological responses from physiological (e.g., Del Rosario et al., 2015) and behavioral (e.g., Brodin et al. 2013; Dzieweczynski et al., 2016) levels to food webs (e.g., Lagesson et al., 2016; Richmond et al., 2018) and ecosystems (e.g., Rosi-Marshal et al., 2013). Although our study was not designed to evaluate the toxicological effects of PPCPs themselves, future studies could usefully address toxicological effects of PPCPs on nearshore Baikal biota by using sewage gradients as *in situ* mesocosms.

In contrast to PPCP concentrations and $\delta^{15}N$ values, microplastics were not associated with IDW population and may be poor proxies for sewage pollution in Lake Baikal. Additionally, microplastics may originate from non-sewage sources, such as agriculture (Steinmetz et al., 2016) and fish nets (Eerkes-Medrano et al. 2015). Because of their long degradation time (Brandon et al. 2016), microplastics can indicate accumulated pollution, which likely promotes wider distribution from nearshore inputs to the offshore (Hendrickson et al., 2018; Fischer et al., 2016). Unlike microplastic concentrations identified in Lake Hovsgol (Free et al. 2014), Lake Superior (Hendrickson et al., 2018), or Lake Erie (Eriksen et al., 2013), microplastic concentrations in Baikal, as quantified by our methods, may be poor proxies for capturing pollution from seasonally varying human populations. It is worth noting that since the time of our field sampling, evidence has accumulated that our methods likely dramatically underestimated microplastic abundance (Wang and Wang 2018; Brandon et al. 2020), and there is potential for the microplastics themselves to cause deleterious ecological responses. While we focus here on microplastics as an indicator of sewage pollution, microplastics are increasingly shown to disrupt food web dynamics by altering grazing patterns (Green 2016) and providing carbon substrate for microbial growth (Romera-Castillo et al. 2018). Together these growing uncertainties suggest that microplastic pollution in Baikal and elsewhere deserves increased attention.

Relating sewage indicators with benthic algal communities

Congruent with our hypotheses, increasing sewage indicators tended to be associated with higher relative abundance of filamentous taxa in periphyton. Previous studies investigating Baikal's periphyton composition noted that areas adjacent to human development often had increased abundance of filamentous algae such as *Ulothrix* and *Spirogyra* (Timoshkin et al. 2016, 2018). Lake Baikal's southwestern shore historically experiences short *Ulothrix* blooms in late August (Kozhov 1963), potentially confounding sewage signals with an annually occurring phenomenon. Our data are consistent with the results of Timoshkin et al. (2016) and show that relative abundance of filamentous algae is greatest near areas of higher lakeside development.

While community composition shifted with increasing sewage indicator concentrations, periphyton $\delta^{15}N$ values did not differ along our transect. Previous studies in marine (Gartner et al. 2002; Savage and Elmgren 2004; Risk et al. 2009) and freshwater (Wayland and Hobson 2001; Camilleri and Ozersky 2019) systems have highlighted how sewage-associated $\delta^{15}N$ can increase in algal samples and even throughout the food web. Like PPCPs in our study, $\delta^{15}N$ values are often most enriched near the source of sewage pollution and can decrease over several kilometers (Savage and Elmgren 2004), with concentrations varying based off species-specific uptake rates and advective, dispersive, and diffusive transport (Gartner et al. 2002). While previous studies using $\delta^{15}N$ signatures in macroalgae and vascular macrophytes have successfully tracked sewage gradients (Cole et al. 2004), periphyton $\delta^{15}N$ as a sewage indicator potentially can be confounded by terrestrial $\delta^{15}N$ contributions such as through agricultural runoff (Chang et al. 2012). In our study, periphyton $\delta^{15}N$ signatures may be explained by periphyton's typically high cell turnover rates (e.g., days; Swamikannu and Hoagland 1989) dampening isotopic patterns, $\delta^{15}N$-accumulating algal taxa being grazed more readily by macroinvertebrates (Rosenberger et al. 2008), or co-limitation dynamics between ammonium and nitrate (York et al. 2007; Piñón-Gimate et al. 2009).

Fatty acid analyses suggested that changes in periphyton community composition altered the nutritional quality of periphyton across the pollution gradient. Periphyton fatty acid profiles from sites with higher sewage pollution had higher levels of 18:3ω3, 18:1ω9, 18:2ω6, and 16:0 relative to 20:5ω3, 16:1ω7, 16:0, and 14:0 fatty acids. This pattern likely reflects the higher abundance of green algae relative to diatoms (Iverson et al. 2004; Osipova et al. 2009; Taipale et al. 2013; Galloway and Winder 2015), which we observed from our periphyton community composition analysis (Figure 3). Together, our periphyton composition and fatty acid results suggest that Baikal's nearshore periphyton communities near human lakeside developments are more dominated by filamentous green algae, and therefore, with lower nutritional content.

Among the array of fatty acids synthesized in algal communities, essential fatty acids (EFAs) are most likely to be taxonomically associated and influenced by changing community composition. EFAs are a subgroup of polyunsaturated fatty acids (PUFAs) that are prone to accumulating in organisms (see Kelly & Scheibling, 2012). Among the eight common EFAs (Taipale et al. 2013), 18:3ω3, 18:2ω6, and 20:5ω3had the highest coefficient of variation between sites. Because these three EFAs demonstrated the greatest variation between sites, our analyses focused on how their relative abundances related to PPCP concentrations and IDW populations. The fatty acids 18:3ω3 and 18:2ω6 have been previously associated with filamentous algae, such as Baikalian *Ulothrix* (Osipova et al. 2009), whereas 20:5ω3 have previously been associated with Baikalian diatoms (Shishlyannikov et al. 2018). Comparing the ratio of filamentous green algae to diatoms could therefore function as proxy for each algal taxon's relative abundance and potentially offer insights into feeding patterns for the grazers.

673
674 *Relating sewage indicators with macroinvertebrate feeding guilds*
675
676 In assessing benthic consumer communities' responses to changing periphyton, our data suggest
677 macroinvertebrate guilds reshape with increasing sewage pollution. Our results support the
678 general conclusion of Timoshkin et al. (2016) that Baikalian mollusc abundance tends to
679 decrease with increasing sewage pollution. Decreased mollusc abundance may have several
680 causes, including low tolerance for increased concentrations of PPCPs or other components of
681 sewage (e.g., Hollingsworth et al. 2002, Timoshkin et al. 2016), inability to consume filamentous
682 algae (Mazzella and Russo 1989), or filamentous algae not offering the proper nutrition (Lowe
683 and Hunter 1988). In contrast to molluscs, amphipods were generally prevalent at all littoral sites
684 regardless of sewage indicator concentrations. *Brandtia* spp. was the only species less abundant
685 with sewage indicator signals. This genus tends to be associated with endemic sponges
686 (Taakhteev & Didorenko, 2015), which may also be decreasing in abundance near areas of
687 lakeside development (Timoshkin et al., 2016). *Eulimnogammarus* spp., one of the most speciose
688 Baikal genera (Tachteev & Didorenko, 2015), was prevalent at all sites, and $\delta^{15}N$ values in its
689 tissue increased slightly but significantly with increasing IDW population. Unlike periphyton,
690 amphipods' increasing $\delta^{15}N$ values may relate to amphipods having longer cellular turnover rates
691 (e.g., weeks; McIntyre and Flecker 2006) relative to periphyton. Consequently, amphipods'
692 enhanced $\delta^{15}N$ values suggest that sewage-derived nutrients are being incorporated into the food
693 web. While we did not test amphipod tissues for other sewage indicators such as PPCPs and
694 microplastics, the potential for PPCPs to bioaccumulate and biomagnify in food webs has been
695 demonstrated, with ecological ramifications remaining uncertain (Lagesson et al., 2016;
696 Richmond et al., 2018). These combined results suggest that mollusc abundance and amphipod
697 $\delta^{15}N$ values may be longer-term indicators of sewage pollution in Baikal.
698
699 In contrast to variation in $\delta^{15}N$ values, amphipod fatty acid profiles did not differ markedly
700 between sites (Figure 7). Amphipods from all collected sites expressed consistent 20:5ω3,
701 22:5ω3, and 22:6ω3 signatures relative to 18:3ω3 and 18:4ω3. Consumers usually accumulate
702 fatty acids from their food source. Yoshii's (1999) study as well as our own stable isotope data
703 suggest that Baikal's benthic, littoral amphipods are likely a combination or grazers and
704 omnivores. Because fatty acid profiles in amphipods largely reflected fatty acid signatures in
705 periphyton, our data suggest that amphipods likely continue grazing on periphyton, despite the
706 food resource changing in community composition and nutritional content. As a consequence,
707 amphipods may be compensating for the shifting nutritional quality of periphyton through at
708 least two potential mechanisms. First, amphipods may selectively consume diatoms as opposed
709 to filamentous algae, meaning diatom relative abundance could decrease both from increased
710 grazing and lesser efficiency at taking up nutrients relative to filamentous taxa. Second,
711 amphipods themselves (e.g., Desvilettes et al. 1997; Castell et al. 2004) or heterotrophic
712 symbionts (Klein Breteler et al. 1999; Veloza et al. 2006; Hiltunen et al. 2017) may upgrade fatty

acids by investing energy to convert C18 fatty acids to C20 and C22 fatty acids. Regardless of the exact mechanism, our data suggest that food web interactions would change with increasing sewage pollution and may imply a net energetic cost through amphipods' differential grazing patterns.

Conclusions

Over the past decade, Lake Baikal has shown signs of nearshore eutrophication, despite the pelagic zone remaining ultra-oligotrophic. While Baikal receives nutrients from multiple sources, sewage-specific indicators used in this study implicate wastewater pollution as one of the sources. Our results corroborate work by Timoshkin et al. (2016, 2018), demonstrating how patchy hot spots of lakeside development at Baikal can create gradients in sewage concentrations and ecological responses. Unlike previous studies, our approach pairs community abundance data (i.e., periphyton and macroinvertebrate counts) and nuanced dietary tracers (i.e., fatty acids) to assess benthic community and food web consequences of sewage pollution. While sewage pollution may lead to changing resources for macroinvertebrate grazers, Baikal's amphipods appear to be compensating either (1) by selectively grazing on diatoms or (2) by consuming less desirable food and upgrading fatty acids. In both cases, our results suggest shifting community interactions and may imply a net energetic cost for amphipods, as they expend energy either by foraging selectively for diatoms or by catabolizing certain essential fatty acids.

Future trajectories: a call for increased nearshore monitoring

Our results underscore the importance of nearshore monitoring in detecting sewage pollution in large lakes. Lake Baikal is considered ultra-oligotrophic based on pelagic sampling (Yoshida et al. 2003; O'Donnell et al. 2017), but nearshore hot spots of eutrophication are developing throughout the lake (Timoshkin et al. 2016, 2018). While pelagic samples are representative of the lake's overall status, nearshore sampling aids managers in identifying pollution loading before the entire system is affected (Jacoby et al. 1991; Lambert et al. 2008; Hampton et al. 2011). Beyond Baikal, several large, deep, oligotrophic lakes have likewise experienced localized sewage pollution with nearshore biological responses, despite pelagic measurements suggesting oligotrophic status (e.g., Jacoby et al. 1991, Rosenberger et al. 2008; Hampton et al., 2011). Once eutrophication of the open water has occurred, mitigation can involve complex socio-economic factors (Carpenter et al. 1999), require system-specific information (Jeppesen et al. 2005), and necessitate long-term strategies (Tong et al. 2020). Because nutrients may enter systems from numerous sources, incorporating sewage specific indicators, such as PPCPs, may be necessary. PPCP sampling has the potential to not only identify sewage-associated nutrient pollution but also assess heterogeneities in sewage loading along a shoreline. When PPCP data are paired with co-located benthic community composition and food web data, managers can take system-specific actions to mitigate ecological consequences before sewage concentrations

753 are detected throughout the lake. Across larger spatial and temporal scales, these paired PPCP-
754 biological samples have potential to offer a synoptic view of the impacts of sewage pollution,
755 enabling regional and local monitoring to coordinate mitigation strategies
756

Works Cited

Anderson, M. J. 2001. A new method for non-parametric multivariate analysis of variance. Austral Ecology **26**: 32–46. doi:10.1111/j.1442-9993.2001.01070.pp.x

Andersson, E., and A.-K. Brunberg. 2006. Inorganic nutrient acquisition in a shallow clearwater lake – dominance of benthic microbiota. Aquatic Sciences **68**: 172–180. doi:10.1007/s00027-006-0805-x

Barnes, D. K. A., F. Galgani, R. C. Thompson, and M. Barlaz. 2009. Accumulation and fragmentation of plastic debris in global environments. Philos Trans R Soc Lond B Biol Sci **364**: 1985–1998. doi:10.1098/rstb.2008.0205

Bendz, D., N. A. Paxéus, T. R. Ginn, and F. J. Loge. 2005. Occurrence and fate of pharmaceutically active compounds in the environment, a case study: Höje River in Sweden. Journal of Hazardous Materials **122**: 195–204. doi:10.1016/j.jhazmat.2005.03.012

Brandon, J. A., A. Freibott, and L. M. Sala. 2020. Patterns of suspended and salp-ingested microplastic debris in the North Pacific investigated with epifluorescence microscopy. Limnology and Oceanography Letters **5**: 46–53. doi:10.1002/lol2.10127

Brandon, J., M. Goldstein, and M. D. Ohman. 2016. Long-term aging and degradation of microplastic particles: Comparing in situ oceanic and experimental weathering patterns. Marine Pollution Bulletin **110**: 299–308. doi:10.1016/j.marpolbul.2016.06.048

Camilleri, A. C., and T. Ozersky. 2019. Large variation in periphyton δ13C and δ15N values in the upper Great Lakes: Correlates and implications. Journal of Great Lakes Research **45**: 986–990. doi:10.1016/j.jglr.2019.06.003

Carpenter, S. R., D. Ludwig, and W. A. Brock. 1999. Management of Eutrophication for Lakes Subject to Potentially Irreversible Change. Ecological Applications **9**: 751–771. doi:10.2307/2641327

784 Castell, J. D., E. J. Kennedy, S. M. C. Robinson, G. J. Parsons, T. J. Blair, and E. Gonzalez-
785 Duran. 2004. Effect of dietary lipids on fatty acid composition and metabolism in juvenile
786 green sea urchins (Strongylocentrotus droebachiensis). Aquaculture **242**: 417–435.
787 doi:10.1016/j.aquaculture.2003.11.003
788 Chang, H.-Y., S.-H. Wu, K.-T. Shao, and others. 2012. Longitudinal variation in food sources
789 and their use by aquatic fauna along a subtropical river in Taiwan. Freshwater Biology
790 **57**: 1839–1853. doi:10.1111/j.1365-2427.2012.02843.x
791 Cole, M. L., I. Valiela, K. D. Kroeger, and others. 2004. Assessment of a delta15N isotopic
792 method to indicate anthropogenic eutrophication in aquatic ecosystems. J. Environ.
793 Qual. **33**: 124–132. doi:10.2134/jeq2004.1240
794 Costanzo, S. D., M. J. O'Donohue, W. C. Dennison, N. R. Loneragan, and M. Thomas. 2001. A
795 New Approach for Detecting and Mapping Sewage Impacts. Marine Pollution Bulletin **42**:
796 149–156. doi:10.1016/S0025-326X(00)00125-9
797 Craine, J. M., A. J. Elmore, L. Wang, and others. 2018. Isotopic evidence for oligotrophication of
798 terrestrial ecosystems. Nature Ecology & Evolution **2**: 1735–1744. doi:10.1038/s41559-
799 018-0694-0
800 Czekalski, N., R. Sigdel, J. Birtel, B. Matthews, and H. Bürgmann. 2015. Does human activity
801 impact the natural antibiotic resistance background? Abundance of antibiotic resistance
802 genes in 21 Swiss lakes. Environment International **81**: 45–55.
803 doi:10.1016/j.envint.2015.04.005
804 Dalsgaard, J., M. St. John, G. Kattner, D. Müller-Navarra, and W. Hagen. 2003. Fatty acid
805 trophic markers in the pelagic marine environment, p. 225–340. *In* Advances in Marine
806 Biology. Elsevier.
807 Desvilettes, Ch., G. Bourdier, and J. Ch. Breton. 1997. On the occurrence of a possible
808 bioconversion of linolenic acid into docosahexaenoic acid by the copepod *Eucyclops*
809 *serrulatus* fed on microalgae. J Plankton Res **19**: 273–278. doi:10.1093/plankt/19.2.273

Eerkes-Medrano, D., R. C. Thompson, and D. C. Aldridge. 2015. Microplastics in freshwater systems: A review of the emerging threats, identification of knowledge gaps and prioritisation of research needs. Water Research **75**: 63–82. doi:10.1016/j.watres.2015.02.012

Focazio, M. J., D. W. Kolpin, K. K. Barnes, E. T. Furlong, M. T. Meyer, S. D. Zaugg, L. B. Barber, and M. E. Thurman. 2008. A national reconnaissance for pharmaceuticals and other organic wastewater contaminants in the United States - II) Untreated drinking water sources. SCIENCE OF THE TOTAL ENVIRONMENT **402**: 201–216. doi:10.1016/j.scitotenv.2008.02.021

Free, C. M., O. P. Jensen, S. A. Mason, M. Eriksen, N. J. Williamson, and B. Boldgiv. 2014. High-levels of microplastic pollution in a large, remote, mountain lake. Marine Pollution Bulletin **85**: 156–163. doi:10.1016/j.marpolbul.2014.06.001

Galloway, A. W. E., and M. Winder. 2015. Partitioning the Relative Importance of Phylogeny and Environmental Conditions on Phytoplankton Fatty Acids. PLOS ONE **10**: e0130053. doi:10.1371/journal.pone.0130053

Galloway, J. N., F. J. Dentener, D. G. Capone, and others. 2004. Nitrogen Cycles: Past, Present, and Future. Biogeochemistry **70**: 153–226. doi:10.1007/s10533-004-0370-0

Gartner, A., P. Lavery, and A. J. Smit. 2002. Use of delta N-15 signatures of different functional forms of macroalgae and filter-feeders to reveal temporal and spatial patterns in sewage dispersal. Mar. Ecol.-Prog. Ser. **235**: 63–73. doi:10.3354/meps235063

Green, D. S. 2016. Effects of microplastics on European flat oysters, Ostrea edulis and their associated benthic communities. Environmental Pollution **216**: 95–103. doi:10.1016/j.envpol.2016.05.043

Guzzo, M. M., G. D. Haffner, S. Sorge, S. A. Rush, and A. T. Fisk. 2011. Spatial and temporal variabilities of δ13C and δ15N within lower trophic levels of a large lake: implications for

estimating trophic relationships of consumers. Hydrobiologia **675**: 41–53. doi:10.1007/s10750-011-0794-1

Hadwen, W. L., and S. E. Bunn. 2005. Food web responses to low-level nutrient and^ 1^ 5N-tracer additions in the littoral zone of an oligotrophic dune lake. Limnology and Oceanography **50**: 1096.

Hampton, S. E., S. C. Fradkin, P. R. Leavitt, and E. E. Rosenberger. 2011. Disproportionate importance of nearshore habitat for the food web of a deep oligotrophic lake. Marine and Freshwater Research **62**: 350. doi:10.1071/MF10229

Hampton, S. E., S. McGowan, T. Ozersky, and others. 2018. Recent ecological change in ancient lakes. Limnology and Oceanography **63**: 2277–2304. doi:10.1002/lno.10938

Hiltunen, M., M. Honkanen, S. Taipale, U. Strandberg, and P. Kankaala. 2017. Trophic upgrading via the microbial food web may link terrestrial dissolved organic matter to Daphnia. J Plankton Res **39**: 861–869. doi:10.1093/plankt/fbx050

Hollingsworth, R. G., J. W. Armstrong, and E. Campbell. 2002. Caffeine as a repellent for slugs and snails. Nature **417**: 915–916. doi:10.1038/417915a

Interfax-Tourism. 2018. Байкал с января по август 2018 года посетили 1,2 миллиона туристов (1.2 million tourists vistied Baikal from January through August 2018). Interfax-Tourism, October 25

Iverson, S. J., C. Field, W. D. Bowen, and W. Blanchard. 2004. Quantitative Fatty Acid Signature Analysis: A New Method of Estimating Predator Diets. Ecological Monographs **74**: 211–235. doi:10.1890/02-4105

Jacoby, J. M., D. D. Bouchard, and C. R. Patmont. 1991. Response of Periphyton to Nutrient Enrichment in Lake Chelan, WA. Lake and Reservoir Management **7**: 33–43. doi:10.1080/07438149109354252

859 Jeppesen, E., M. Søndergaard, J. P. Jensen, and others. 2005. Lake responses to reduced
860 nutrient loading – an analysis of contemporary long-term data from 35 case studies.
861 Freshwater Biology **50**: 1747–1771. doi:10.1111/j.1365-2427.2005.01415.x
862 Johnson, R. A., and D. V. Wichern. 2007. Applied Multivariate Statistical Analysis, 6th ed.
863 Prentice Hall.
864 Kaufman, L., and P. J. Rousseeuw. 2005. Finding Groups in Data: An Introduction to Cluster
865 Analysis, 1st Edition. Wiley-Interscience.
866 Kelly, J. R., and R. E. Scheibling. 2012. Fatty acids as dietary tracers in benthic food webs.
867 Marine Ecology Progress Series **446**: 1–22. doi:10.3354/meps09559
868 Klein Breteler, W. C. M., N. Schogt, M. Baas, S. Schouten, and G. W. Kraay. 1999. Trophic
869 upgrading of food quality by protozoans enhancing copepod growth: role of essential
870 lipids. Marine Biology **135**: 191–198. doi:10.1007/s002270050616
871 Klein, S., E. Worch, and T. P. Knepper. 2015. Occurrence and Spatial Distribution of
872 Microplastics in River Shore Sediments of the Rhine-Main Area in Germany. Environ.
873 Sci. Technol. **49**: 6070–6076. doi:10.1021/acs.est.5b00492
874 Kolpin, D. W., E. T. Furlong, M. T. Meyer, E. M. Thurman, S. D. Zaugg, L. B. Barber, and H. T.
875 Buxton. 2002. Pharmaceuticals, Hormones, and Other Organic Wastewater
876 Contaminants in U.S. Streams, 1999−2000: A National Reconnaissance. Environmental
877 Science & Technology **36**: 1202–1211. doi:10.1021/es011055j
878 Kozhov, M. M. 1963. Lake Baikal and its Life, Springer Science & Business Media.
879 Kozhova, O. M., and L. R. Izmest'eva. 1998. Lake Baikal: Evolution and Biodiversity, Backhuys
880 Publishers.
881 Kravtsova, L. S., L. A. Izhboldina, I. V. Khanaev, and others. 2014. Nearshore benthic blooms of
882 filamentous green algae in Lake Baikal. Journal of Great Lakes Research **40**: 441–448.
883 doi:10.1016/j.jglr.2014.02.019

884 Lambert, D., A. Cattaneo, and R. Carignan. 2008. Periphyton as an early indicator of
885 perturbation in recreational lakes. Can. J. Fish. Aquat. Sci. **65**: 258–265.
886 doi:10.1139/f07-168
887 Legendre, P., and L. Legendre. 2012. Numerical Ecology, 3rd ed. Elsevier.
888 Li, J., C. Green, A. Reynolds, H. Shi, and J. M. Rotchell. 2018. Microplastics in mussels
889 sampled from coastal waters and supermarkets in the United Kingdom. Environmental
890 Pollution **241**: 35–44. doi:10.1016/j.envpol.2018.05.038
891 Lowe, R. L., and R. D. Hunter. 1988. Effect of Grazing by Physa integra on Periphyton
892 Community Structure. Journal of the North American Benthological Society **7**: 29–36.
893 doi:10.2307/1467828
894 Mazzella, L., and G. F. Russo. 1989. Grazing effect of two Gibbula species (Mollusca,
895 Archaeogastropoda) on the epiphytic community of Posidonia oceanica leaves.
896 McIntyre, P. B., and A. S. Flecker. 2006. Rapid turnover of tissue nitrogen of primary consumers
897 in tropical freshwaters. Oecologia **148**: 12–21. doi:10.1007/s00442-005-0354-3
898 Meyer, M. F., S. M. Powers, and S. E. Hampton. 2019. An Evidence Synthesis of
899 Pharmaceuticals and Personal Care Products (PPCPs) in the Environment: Imbalances
900 among Compounds, Sewage Treatment Techniques, and Ecosystem Types. Environ.
901 Sci. Technol. **53**: 12961–12973. doi:10.1021/acs.est.9b02966
902 Monteith, D. T., J. L. Stoddard, C. D. Evans, and others. 2007. Dissolved organic carbon trends
903 resulting from changes in atmospheric deposition chemistry. Nature **450**: 537–540.
904 doi:10.1038/nature06316
905 Moore, M. V., S. E. Hampton, L. R. Izmest'eva, E. A. Silow, E. V. Peshkova, and B. K. Pavlov.
906 2009. Climate Change and the World's "Sacred Sea"-Lake Baikal, Siberia. Bioscience
907 **59**: 405–417. doi:10.1525/bio.2009.59.5.8

908 Moran, P. W., S. E. Cox, S. S. Embrey, R. L. Huffman, T. D. Olsen, and S. C. Fradkin. 2012.
909 Sources and Sinks of Nitrogen and Phosphorus in a Deep, Oligotrophic Lake, Lake
910 Crescent, Olympic National Park, Washington. US Geological Survey.
911 O'Donnell, D. R., P. Wilburn, E. A. Silow, L. Y. Yampolsky, and E. Litchman. 2017. Nitrogen and
912 phosphorus colimitation of phytoplankton in Lake Baikal: Insights from a spatial survey
913 and nutrient enrichment experiments. Limnology and Oceanography **62**: 1383–1392.
914 doi:10.1002/lno.10505
915 Oksanen, J., F. G. Blanchet, M. Friendly, and others. 2019. vegan: Community Ecology
916 Package,.
917 Osipova, S., L. Dudareva, N. Bondarenko, A. Nasarova, N. Sokolova, L. Obolkina, O. Glyzina,
918 and O. Timoshkin. 2009. Temporal variation in fatty acid composition of Ulothrix zonata
919 (Chlorophyta) from ice and benthic communities of Lake Baikal. Phycologia **48**: 130–
920 135.
921 Ozersky, T., E. A. Volkova, N. A. Bondarenko, O. A. Timoshkin, V. V. Malnik, V. M. Domysheva,
922 and S. E. Hampton. 2018. Nutrient limitation of benthic algae in Lake Baikal, Russia.
923 Freshwater Science **37**: 472–482. doi:10.1086/699408
924 Piñón-Gimate, A., M. F. Soto-Jiménez, M. J. Ochoa-Izaguirre, E. García-Pagés, and F. Páez-
925 Osuna. 2009. Macroalgae blooms and δ15N in subtropical coastal lagoons from the
926 Southeastern Gulf of California: Discrimination among agricultural, shrimp farm and
927 sewage effluents. Marine Pollution Bulletin **58**: 1144–1151.
928 doi:10.1016/j.marpolbul.2009.04.004
929 Powers, S. M., T. W. Bruulsema, T. P. Burt, and others. 2016. Long-term accumulation and
930 transport of anthropogenic phosphorus in three river basins. Nature Geoscience **9**: 353–
931 356. doi:10.1038/ngeo2693
932 R Core Team. 2019. R: A Language and Environment for Statistical Computing,.

933 Risk, M. J., B. E. Lapointe, O. A. Sherwood, and B. J. Bedford. 2009. The use of δ15N in
934 assessing sewage stress on coral reefs. Marine Pollution Bulletin **58**: 793–802.
935 doi:10.1016/j.marpolbul.2009.02.008
936 Romera-Castillo, C., M. Pinto, T. M. Langer, X. A. Álvarez-Salgado, and G. J. Herndl. 2018.
937 Dissolved organic carbon leaching from plastics stimulates microbial activity in the
938 ocean. Nat Commun **9**: 1–7. doi:10.1038/s41467-018-03798-5
939 Rosenberger, E. E., S. E. Hampton, S. C. Fradkin, and B. P. Kennedy. 2008. Effects of
940 shoreline development on the nearshore environment in large deep oligotrophic lakes.
941 Freshwater Biology **53**: 1673–1691. doi:10.1111/j.1365-2427.2008.01990.x
942 Rosi-Marshall, E. J., and T. V. Royer. 2012. Pharmaceutical Compounds and Ecosystem
943 Function: An Emerging Research Challenge for Aquatic Ecologists. Ecosystems **15**:
944 867–880. doi:10.1007/s10021-012-9553-z
945 Sargent, J. R., and S. Falk-Petersen. 1988. The lipid biochemistry of calanoid copepods.
946 Hydrobiologia **167–168**: 101–114. doi:10.1007/BF00026297
947 Savage, C., and R. Elmgren. 2004. MACROALGAL (FUCUS VESICULOSUS) δ15N VALUES
948 TRACE DECREASE IN SEWAGE INFLUENCE. Ecological Applications **14**: 517–526.
949 doi:10.1890/02-5396
950 Shishlyannikov, S. M., A. A. Nikonova, Y. S. Bukin, and A. G. Gorshkov. 2018. Fatty acid trophic
951 markers in Lake Baikal phytoplankton: A comparison of endemic and cosmopolitan
952 diatom-dominated phytoplankton assemblages. Ecological Indicators **85**: 878–886.
953 doi:10.1016/j.ecolind.2017.11.052
954 Smith, V. H., G. D. Tilman, and J. C. Nekola. 1999. Eutrophication: impacts of excess nutrient
955 inputs on freshwater, marine, and terrestrial ecosystems. Environmental Pollution **100**:
956 179–196. doi:10.1016/S0269-7491(99)00091-3
957 Sneath, P. H. A., and R. R. Sokal. 1973. Numerical Taxonomy: The Principles and Practice of
958 Numerical Classification, W. H. Freeman.

Stoddard, J. L., J. Van Sickle, A. T. Herlihy, J. Brahney, S. Paulsen, D. V. Peck, R. Mitchell, and A. I. Pollard. 2016. Continental-Scale Increase in Lake and Stream Phosphorus: Are Oligotrophic Systems Disappearing in the United States? Environ. Sci. Technol. **50**: 3409–3415. doi:10.1021/acs.est.5b05950

Swamikannu, X., and K. D. Hoagland. 1989. Effects of Snail Grazing on the Diversity and Structure of a Periphyton Community in a Eutrophic Pond. Can. J. Fish. Aquat. Sci. **46**: 1698–1704. doi:10.1139/f89-215

Taipale, S., U. Strandberg, E. Peltomaa, A. W. E. Galloway, A. Ojala, and M. T. Brett. 2013. Fatty acid composition as biomarkers of freshwater microalgae: analysis of 37 strains of microalgae in 22 genera and in seven classes. Aquatic Microbial Ecology **71**: 165–178. doi:10.3354/ame01671

Timoshkin, O. A., M. V. Moore, N. N. Kulikova, and others. 2018. Groundwater contamination by sewage causes benthic algal outbreaks in the littoral zone of Lake Baikal (East Siberia). Journal of Great Lakes Research. doi:10.1016/j.jglr.2018.01.008

Timoshkin, O. A., D. P. Samsonov, M. Yamamuro, and others. 2016. Rapid ecological change in the coastal zone of Lake Baikal (East Siberia): Is the site of the world's greatest freshwater biodiversity in danger? Journal of Great Lakes Research **42**: 487–497. doi:10.1016/j.jglr.2016.02.011

Tong, Y., M. Wang, J. Peñuelas, and others. 2020. Improvement in municipal wastewater treatment alters lake nitrogen to phosphorus ratios in populated regions. Proc Natl Acad Sci USA **117**: 11566–11572. doi:10.1073/pnas.1920759117

Turetsky, M. R., R. K. Wieder, C. J. Williams, and D. H. Vitt. 2000. Organic matter accumulation, peat chemistry, and permafrost melting in peatlands of boreal Alberta. Écoscience **7**: 115–122. doi:10.1080/11956860.2000.11682608

983 Veloza, A. J., F.-L. E. Chu, and K. W. Tang. 2006. Trophic modification of essential fatty acids
984 by heterotrophic protists and its effects on the fatty acid composition of the copepod
985 Acartia tonsa. Marine Biology **148**: 779–788. doi:10.1007/s00227-005-0123-1
986 Volkova, E. A., N. A. Bondarenko, and O. A. Timoshkin. 2018. Morphotaxonomy, distribution
987 and abundance of *Spirogyra* (Zygnematophyceae, Charophyta) in Lake Baikal, East
988 Siberia. Phycologia **57**: 298–308. doi:10.2216/17-69.1
989 Wang, W., and J. Wang. 2018. Investigation of microplastics in aquatic environments: An
990 overview of the methods used, from field sampling to laboratory analysis. TrAC Trends
991 in Analytical Chemistry **108**: 195–202. doi:10.1016/j.trac.2018.08.026
992 Wayland, M., and K. A. Hobson. 2001. Stable carbon, nitrogen, and sulfur isotope ratios in
993 riparian food webs on rivers receiving sewage and pulp-mill effluents. Can. J. Zool. **79**:
994 5–15. doi:10.1139/z00-169
995 Wickham, H. 2016. ggplot2: Elegant Graphics for Data Analysis, Springer-Verlag.
996 Wickham, H., R. Francois, L. Henry, and K. Mueller. 2019. dplyr: A Grammar of Data
997 Manipulation,.
998 Wickham, H., and L. Henry. 2019. tidyr: Easily Tidy Data with ‘spread()’ and ‘gather()’
999 Functions,.
1000 Yang, Y., W. Song, H. Lin, W. Wang, L. Du, and W. Xing. 2018. Antibiotics and antibiotic
1001 resistance genes in global lakes: A review and meta-analysis. Environment International
1002 **116**: 60–73. doi:10.1016/j.envint.2018.04.011
1003 Yang, Y.-Y., G. S. Toor, P. C. Wilson, and C. F. Williams. 2016. Septic systems as hot-spots of
1004 pollutants in the environment: Fate and mass balance of micropollutants in septic
1005 drainfields. Science of The Total Environment **566–567**: 1535–1544.
1006 doi:10.1016/j.scitotenv.2016.06.043

York, J. K., G. Tomasky, I. Valiela, and D. J. Repeta. 2007. Stable isotopic detection of ammonium and nitrate assimilation by phytoplankton in the Waquoit Bay estuarine system. Limnology and Oceanography **52**: 144–155. doi:10.4319/lo.2007.52.1.0144

Yoshida, T., T. Sekino, M. Genkai-Kato, and others. 2003. Seasonal dynamics of primary production in the pelagic zone of southern Lake Baikal. Limnology **4**: 53–62. doi:10.1007/s10201-002-0089-3

2016a. Methods for determination of nitrogen-containing matters (with corrections) (Методы определения азотсодержащих веществ (с Поправками)).

2016b. Methods for determination of phosphorus-containing matters (with corrections) (Методы определения фосфорсодержащих веществ).

2017. Nitrate concentration in waters: Photometric methods with Giress reagent following stabilization in a cadmium reducer (Массовая концентрация нитратного азота в водах: Методика измерений фотометрическим методом с реактивом Грисса после восстановления в камиевом редукторе).

Acknowledgments

We would like to thank the faculty, students, staff, and mariners of the Irkutsk State University's Biological Research Institute Biostation for their expert field, taxonomic, and laboratory support; Marianne Moore and Bart De Stasio for helpful advice; the researchers and students of the Siberian Branch of the Russian Academy of Sciences Limnological Institute for expert taxonomic and logistical assistance; Stephen M. Powers, Stephanie G. Labou, Stephen L. Katz, Brian P. Lanouette, John R. Loffredo, Alexander K. Fremier, Erica J. Crespi, Daniel L. Preston, and Jim J. Elser for offering insights throughout the development of this project. Funding was provided by the National Science Foundation (NSF-DEB-1136637) to S.E.H., a Fulbright Fellowship to M.F.M., a NSF Graduate Research Fellowship to M.F.M. (NSF-DGE-1347973), and the Russian Ministry of Education and Science Research Project (No. GR 01201461929; 1354-2014/51). This work serves as one chapter of M.F.M.'s doctoral dissertation in Environmental and Natural Resource Sciences at Washington State University.

1037

Table 1: Location, depth, temperature and population information for each of the 17 sampling stations. “OS” refers to pelagic locations (i.e., “Offshore”), whereas other site abbreviations refer to littoral sampling locations.

Site	Latitude	Longitude	Depth (m)	Distance to shore (m)	Air Temperature (C)	Surface Temperature (C)	Adjacent Population
BK-1	51.90316	105.07404	0.7	10	18	14	56
BK-2	51.90365	105.069	0.9	17.5	19	13	56
BK-3	51.90536	105.0957	0.8	10	18	14	56
BGO-1	52.02693	105.40102	0.9	18	20	13	0
BGO-2	52.0197	105.37707	1.1	14	19	14	600
BGO-3	52.02649	105.43577	0.7	21	18	16	600
OS-1	51.98559	105.47237	900	NA	15	NA	NA
KD-1	51.92646	105.24504	0.8	20.75	23	NA	0
KD-2	51.91807	105.21456	0.9	14.5	23	16	0
MS-1	51.89863	105.15017	0.6	10.5	21	17	0
SM-1	51.87152	104.98006	0.9	11.5	21	15	0
LI-1	51.86825	104.83042	0.6	8.9	19	14	2000
LI-2	51.84626	104.87356	0.8	9.4	21	15	2000
LI-3	51.85407	104.86216	0.7	9.25	19.5	15	2000
EM-1	51.86005	104.93999	0.7	15.5	24.5	14	0
OS-2	51.8553	104.8148	1300	NA	21	NA	NA
OS-3	51.859108	105.0769	1400	5000	NA	14.5	NA

1038

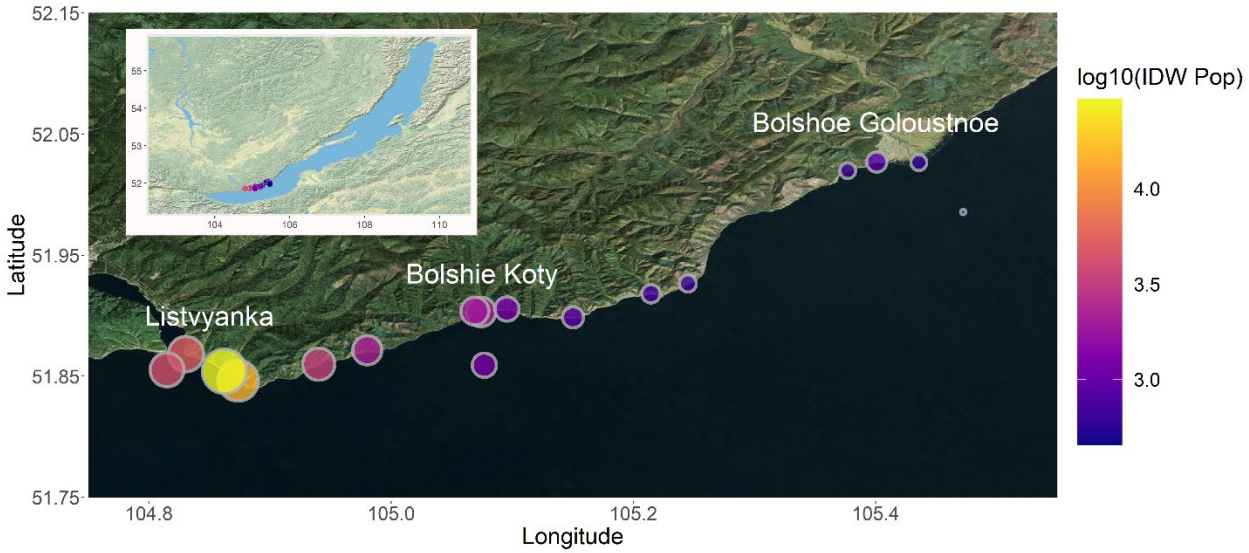

Figure 1: Map of all sampling locations with sites sized and colored by log-transformed IDW population. IDW population was log-transformed so as to make IDW populations across three orders of magnitude more comparable. The entire transect included three developed sites (i.e., Listvyanka, Bolshie Koty, Bolshoe Goloustnoe). Three offshore samples were also collected to compare pelagic sewage signals to those in the littoral. Sampling locations west of Listvyanka are located farther from Listvyanka's centroid, and therefore have lower IDW population values than sites located closer to the centroid.

Figure 2: Photographs and Google Earth imagery of each developed area. Photographs were taken by Kara H. Woo and Michael F. Meyer.

Table 2: Average sewage indicator concentrations and densities per sampling location												
Site	NH_4^+ (mg/L)	NO_3^- (mg/L)	TP (mg/L)	Caffeine (ng/L)	Acetaminophen (ng/L)	Paraxanthine (ng/L)	Cotinine (ng/L)	Fragment density (MPs/L)	Fiber density (MPs/L)	Bead density (MPs/L)	IDW population	Categorical IDW population
BK-1	0.003	0.085	0.054	0.011	0.001	0.002	0	0	0.000833	0	2304.039	High
BK-2	0.003	0.085	0.052	0.007	0.001	0	0	0.000952	0.000476	0	1891.558	Mod
BK-3	0.068	0.09	0.045	0.003	0.001	0	0	0.003095	0.00119	0	1231.234	Mod
BGO-1	0.0145	0.085	0.044	0	0.002	0	0	0.00119	0	0	838.5385	Low
BGO-2	0.001	0.08	0.0385	0	0.001	0	0	0.000238	0.001905	0	611.91	Low
BGO-3	0.001	0.09	0.044	0.005	0.003	0	0	0	0	0	624.455	Low
OS-1	0.001	0.085	0.061	0	0.001	0	0.001	0.002381	0	0	455.7733	Low
KD-1	0.0035	0.065	0.0375	0.003	0.001	0	0	0	0.000476	0	662.4151	Low
KD-2	0.001	0.1	0.0445	0.001	0.001	0	0	0.000714	0.001905	0	720.5484	Low
MS-1	0.001	0.09	0.061	0.064	0.035	0.015	0	0	0.000238	0	903.6733	Low
SM-1	0.001	0.085	0.1475	0.042	0.012	0.005	0	0	0.001667	0	2146.218	Mod
LI-1	0.004	0.08	0.0385	0.05	0.04	0.006	0.002	0.00381	0.000238	0.000714	5403.209	High
LI-2	0.091	0.095	0.0775	0.001	0.007	0	0	0.001429	0.00119	0	14792.51	High
LI-3	0.0035	0.08	0.077	0.027	0.002	0.002	0.003	0.000476	0	0.000714	29511.73	High
EM-1	0.1125	0.185	0.092	0.029	0.014	0.002	0	0	0.000238	0	3389.949	High
OS-2	0.001	0.08	0.078	0.033	0.001	0.004	0.003	0.000238	0.001905	0	4340	High
OS-3	0.001	0.08	0.0795	0.001	0.001	0	0	0	0.002143	0	1221.424	Mod

1054

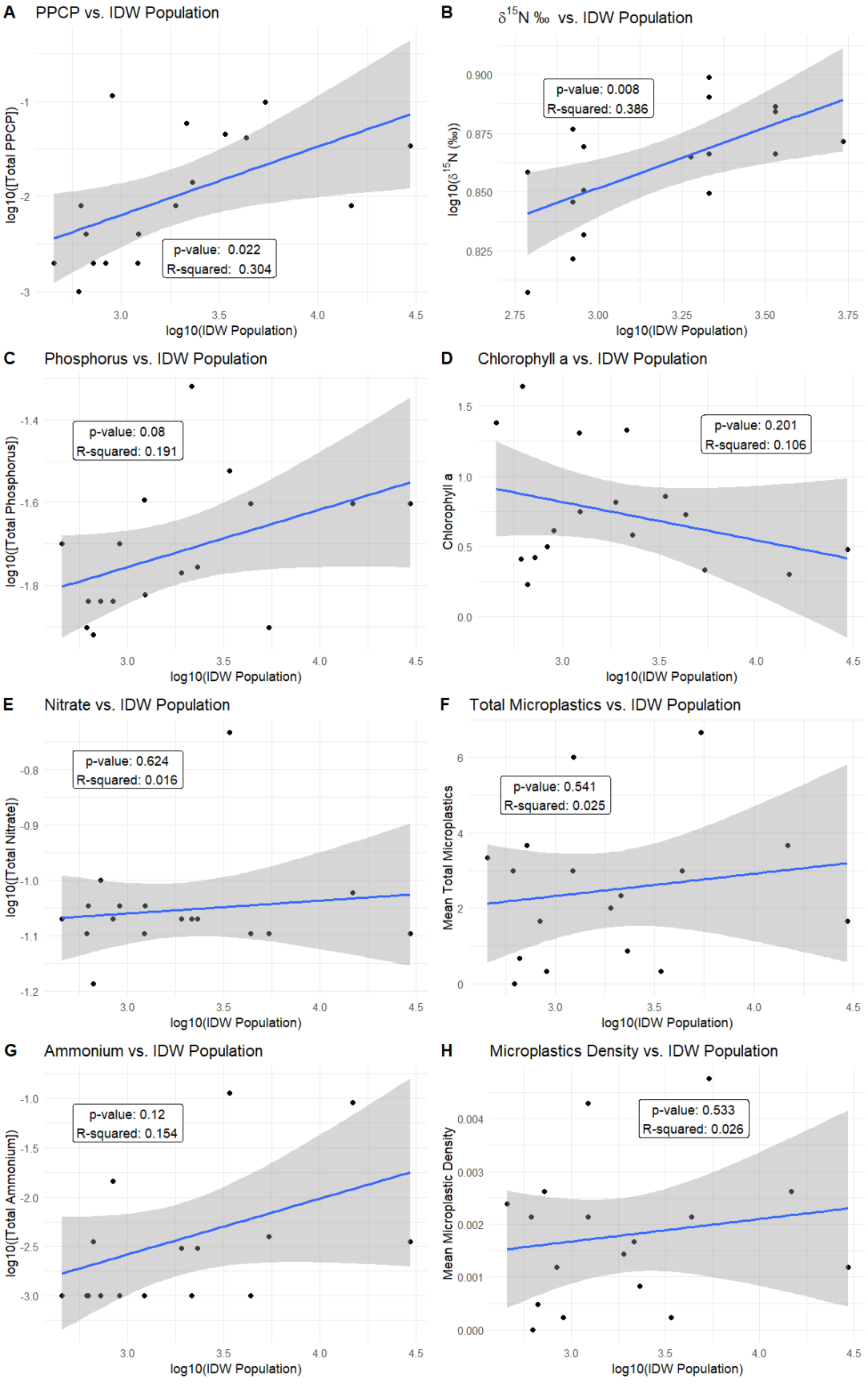
A PPCP vs. IDW Population
log10([Total PPCP])
log10(IDW Population)
p-value: 0.022
R-squared: 0.304
B δ15N ‰ vs. IDW Population
log10(δ15N (‰))
log10(IDW Population)
p-value: 0.008
R-squared: 0.386
C Phosphorus vs. IDW Population
log10([Total Phosphorus])
log10(IDW Population)
p-value: 0.08
R-squared: 0.191
D Chlorophyll a vs. IDW Population
Chlorophyll a
log10(IDW Population)
p-value: 0.201
R-squared: 0.106
E Nitrate vs. IDW Population
log10([Total Nitrate])
log10(IDW Population)
p-value: 0.624
R-squared: 0.016
F Total Microplastics vs. IDW Population
Mean Total Microplastics
log10(IDW Population)
p-value: 0.541
R-squared: 0.025
G Ammonium vs. IDW Population
log10([Total Ammonium])
log10(IDW Population)
p-value: 0.12
R-squared: 0.154
H Microplastics Density vs. IDW Population
Mean Microplastic Density
log10(IDW Population)
p-value: 0.533
R-squared: 0.026

1055

Figure 3: Linear models of total PPCP concentrations (A), macroinvertebrate $\delta^{15}N$ (B), total phosphorus (C), chlorophyll a (D), nitrate (E), total microplastics (F), ammonium (G), and microplastic density (H) regressed against log-transformed inverse distance weighted (IDW) population. Total PPCP concentrations (A) and macroinvertebrate $\delta^{15}N$ (B) produced significant models. Total phosphorus (C), chlorophyll a (D), nitrate (E), total microplastics (F), ammonium (G), and microplastic density (H) did not produce significant models.

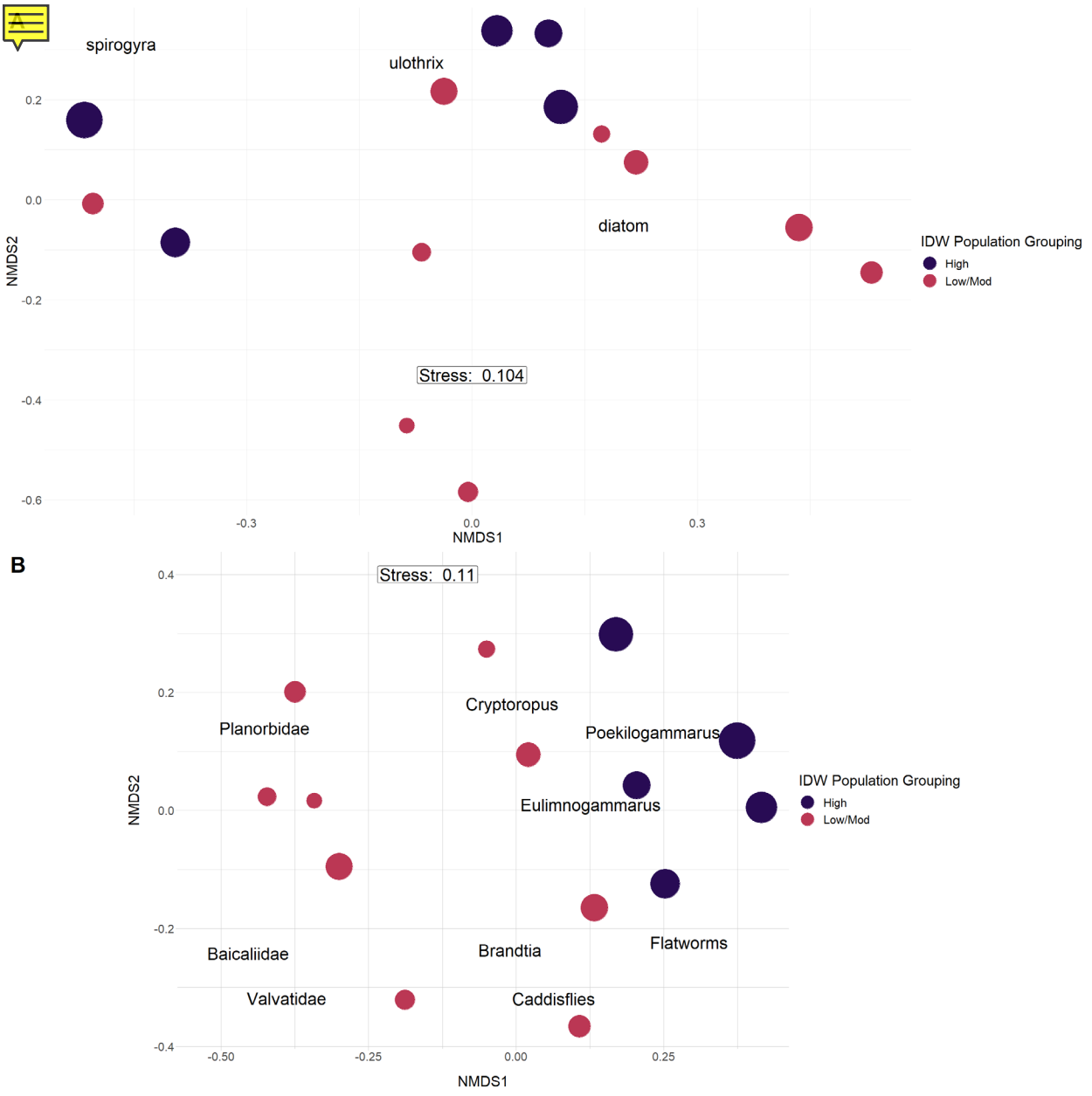

Figure 4: Periphyton (a) and macroinvertebrate (b) abundance NMDS with Bray-Curtis dissimilarity. Points are sized by log10 IDW population and colored by grouped IDW population values. Taxonomic labels represent species scores, which are weighted averages of species contributions from site scores. (a) For periphyton, PERMANOVA ($p = 0.001$) and post-hoc SIMPER results suggested sites with a higher IDW population value tended to be more associated with filamentous algal groupings and separate from sites with moderate and low IDW population values, which were more associated with diatom abundance. (b) For macroinvertebrates, PERMANOVA ($p = 0.02$) and post-hoc SIMPER results suggested sites with a higher IDW population values tended to be associated with amphipod taxa (see Table S1),

whereas sites with lower and moderate IDW population values were more associated with increased mollusc abundance (see Table S1).

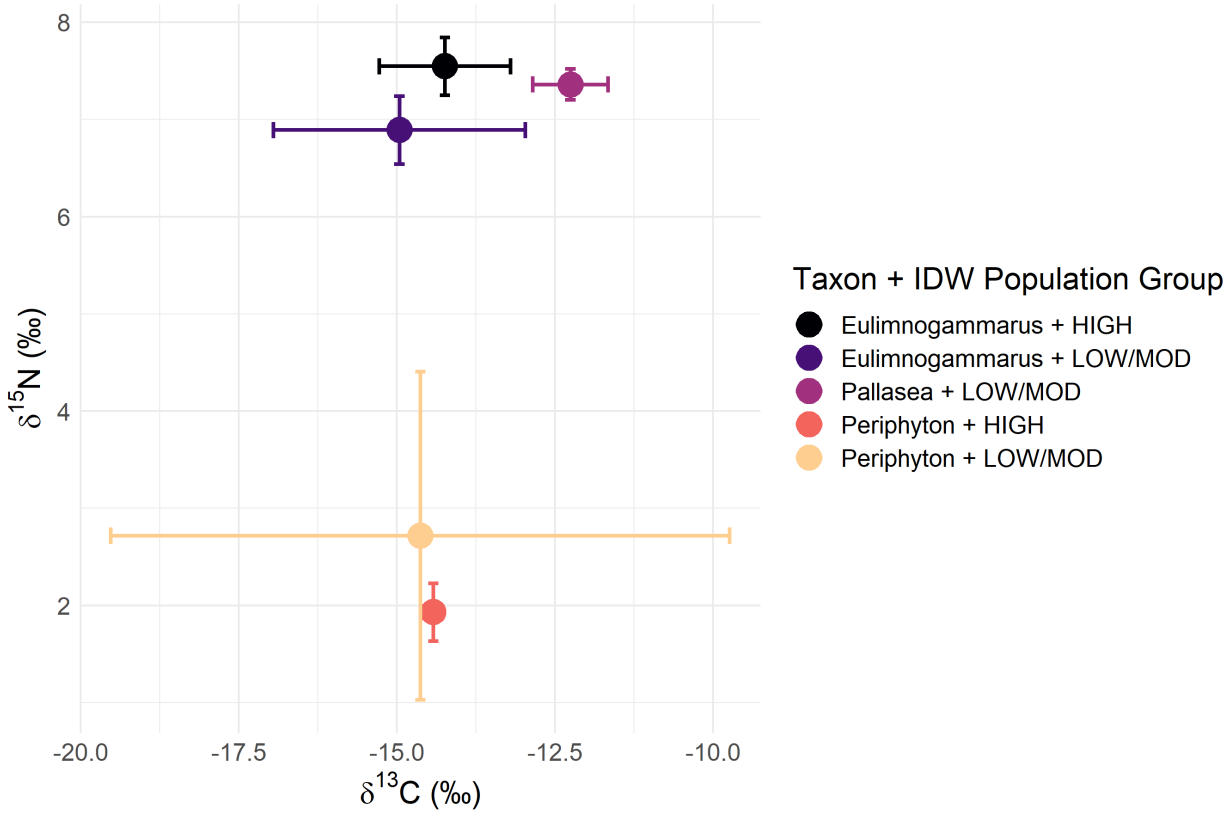

Figure 5: Biplot of mean and standard deviation $\delta^{13}C$ and $\delta^{15}N$ stable isotope values for littoral amphipods and periphyton, grouped by categorical IDW population (Table 3). In general, periphyton did not differ in $\delta^{13}C$ or $\delta^{15}N$ signatures with increasing IDW population, whereas *Eulimnogammarus* amphipods increased in $\delta^{15}N$ signatures with increasing IDW population. *Pallasea* signatures differed from *Eulimnogammarus* most likely because *Pallasea* tends to remain in the nearshore area, whereas *Eulimnogammarus* will regularly migrate to deeper zones (Taakhteev & Didorenko, 2015).

Table 3: Mean inter-site fatty acid proportion of each taxon and fatty acid grouping (as defined in table S2).

Taxon	Number of sites	Branched	LCPUFA	MUFA	SAFA	SCPUFA
Drapa spp.	4	0.000	0.012	0.088	0.189	0.710
Eulimnogammarus cyaneus	2	0.002	0.259	0.309	0.248	0.182
Eulimnogammarus verrucosus	6	0.000	0.188	0.385	0.240	0.187
Eulimnogammarus vittatus	6	0.001	0.171	0.371	0.241	0.216
Pallasea cancellus	3	0.001	0.282	0.359	0.187	0.171
Periphyton	7	0.000	0.073	0.092	0.284	0.550
Snail	3	0.002	0.470	0.123	0.194	0.211

1085

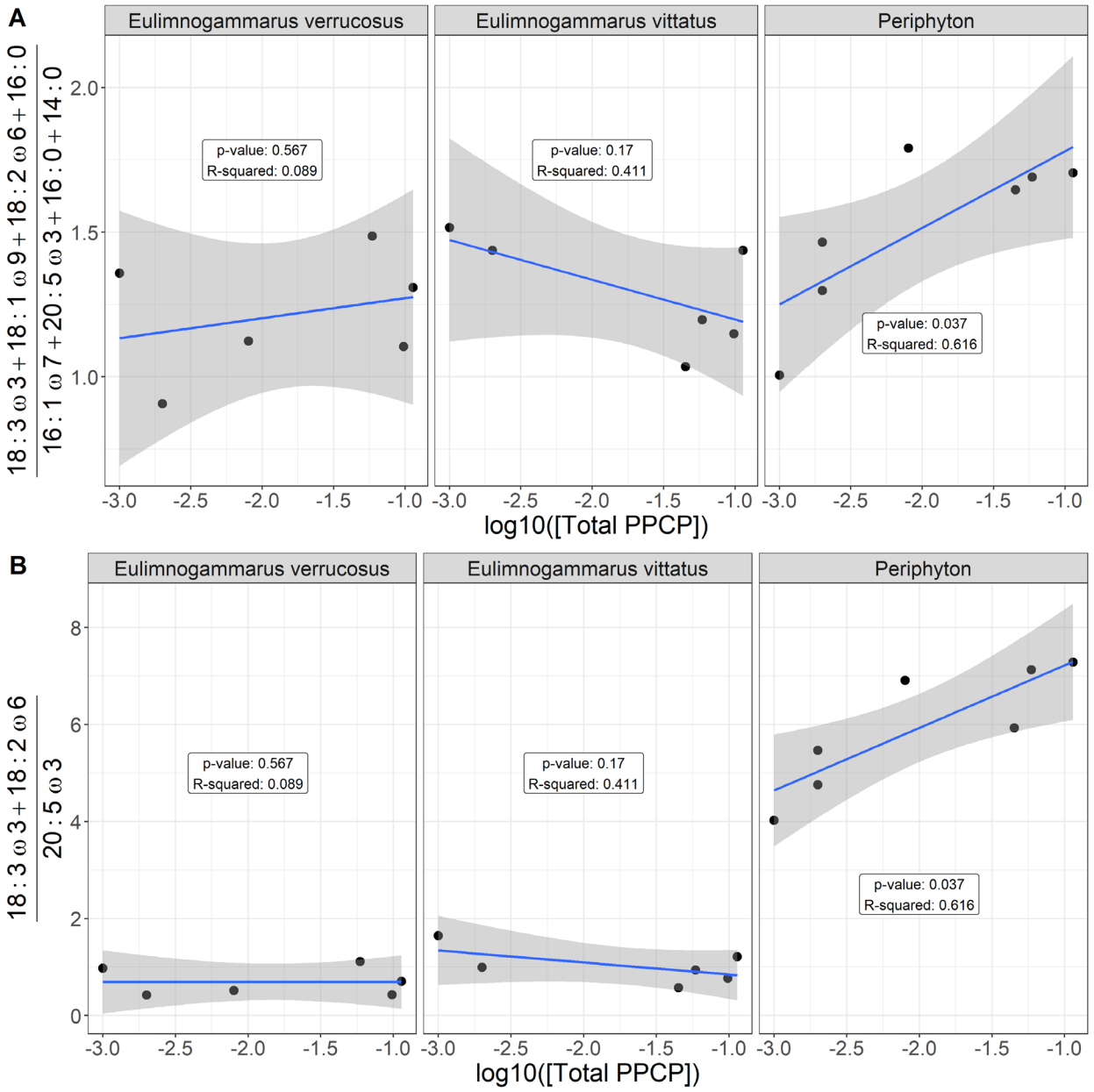

Figure 6: Ratio of filamentous:diatom-associated fatty acids (a) and essential fatty acids (b) across our PPCP gradient. Our first analysis (a) focused solely on green filamentous algal fatty acids (i.e., 18:3ω3, 18:1ω9, 18:2ω6, and 16:0 relative to diatom fatty acids (i.e., 20:5ω3, 16:1ω7, 16:0, 14:0) in relation to increasing PPCP concentrations. This first analysis suggested periphyton reflected an increasing green, filamentous signature relative to diatoms, which corroborates analyses community compositional shifts (Figure 4a). While periphyton fatty acids changed significantly across our sewage gradient, macroinvertebrate signatures remained consistent. Our second analysis (b) focused solely on the essential fatty acids, which further highlights the trends observed in periphyton and macroinvertebrate grazers.

1098

Table S1: Macroinvertebrate taxonomic groupings for abundance estimates. Amphipod taxa were defined as in Taakhteev & Didorenko, 2015; Mollusc taxa were defined as in Sitnikova, 2012.

Amphipoda	Mollusca	Other
Brandtia latissima intermida (Dorogostaiskii 1930)	Acroloxidae	Asellidae
Brandtia latissima lata (Dybowsky 1874)	Baicaliidae	Caddisflies
Brandtia latissima latior (Dybowsky 1874)	Benedictidate	Hirudinea
Brandtia latissima latissima (Gerstfeldt 1858)	Maackia	Planaria
Brandtia parasitica parasitica (Dybowsky 1874)	Planorbidae	
Cryptoropus inflatus (Dybowsky 1874)	Valvatidae	
Cryptoropus pachytus (Dybowsky 1874)		
Cryptoropus rugosus (Dybowsky 1874)		
Eulimnogammarus capreolus (Dybowsky 1874)		
Eulimnogammarus cruentes (Dorogostaiskii 1930)		
Eulimnogammarus cyaneus (Dybowsky 1874)		
Eulimnogammarus grandimanus (Bazikalova 1945)		
Eulimnogammarus maacki (Gerstfeldt 1858)		
Eulimnogammarus marituji (Bazikalova 1945)		
Eulimnogammarus verucossus (Gerstfeldt 1858)		
Eulimnogammarus viridis viridis (Dybowsky 1874)		
Eulimnogammarus vittatus (Dybowsky 1874)		
Pallasea brandtia brandita (Dybowsky 1874)		
Pallasea brandtii tenera (Sovinskii 1930)		
Pallasea cancelloides (Gerstfeldt 1858)		
Pallasea cancellus (Pallas 1776)		
Pallasea viridis (Garjajev 1901)		
Poekilogammarus crassimus (Sovinskii 1915)		
Poekilogammarus ephippiatus (Dybowsky 1874)		
Poekilogammarus megonychus perpolitus (Takhteev 2002)		
Poekilogammarus pictus (Dybowsky 1874)		

1099

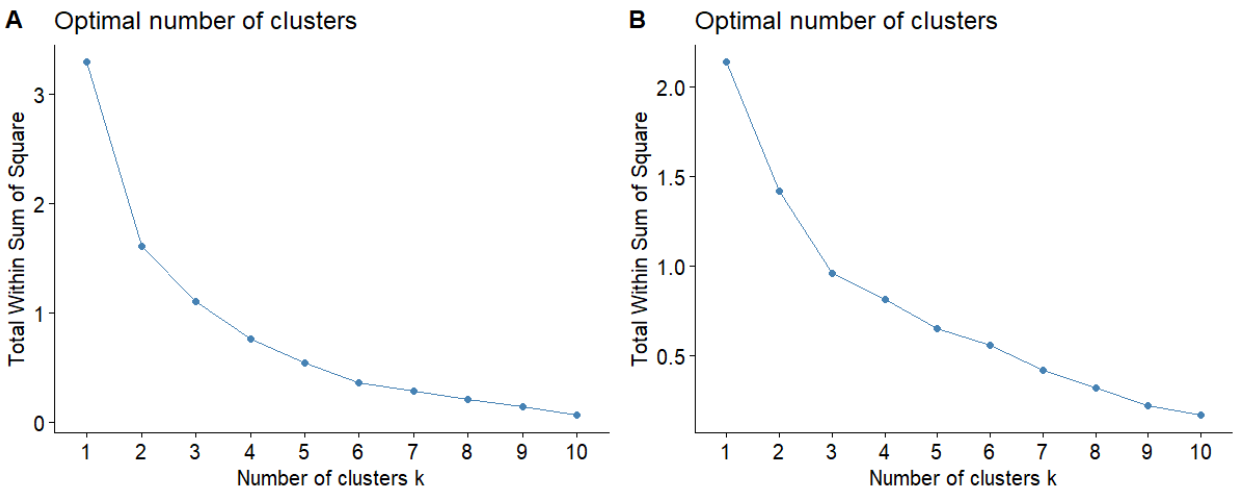

Figure S1: With-group-sum-of-squares (wss) for increasing number of k-mediod clusters for periphyton (A) and invertebrate (B) community data. In the case of periphyton data, wss decreases most markedly with three clusters, whereas invertebrate community abundance is best described by potential two or three clusters.

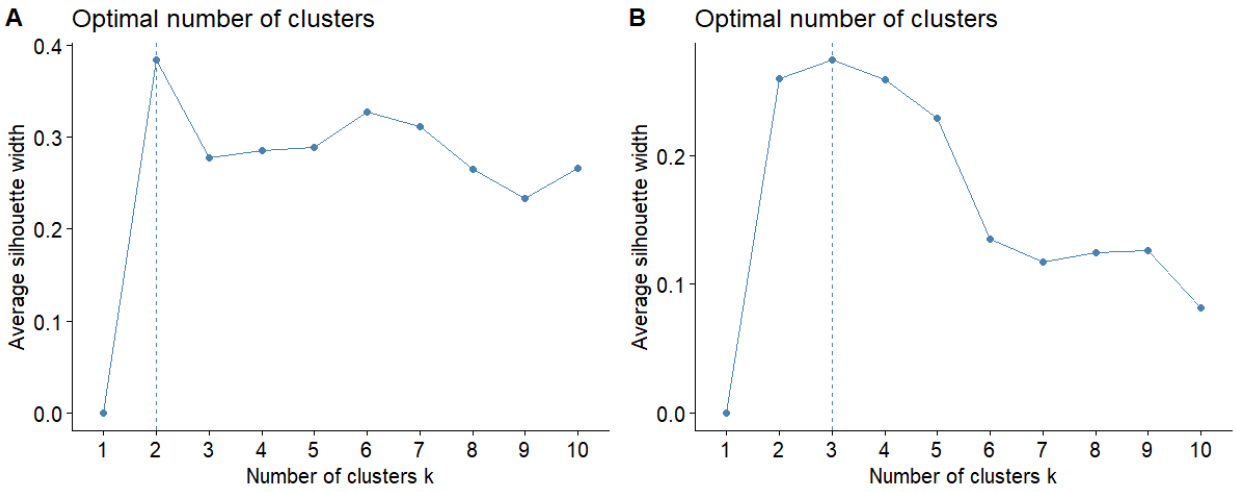

Figure S2: Average silhouette width for increasing number of k-mediod clusters for periphyton (A) and invertebrate (B) community data. In the case of periphyton data, average silhouette width decreases most markedly with three clusters, whereas invertebrate community abundance is best described by two or three clusters as the average silhoette width for both two and three clusters was highest below beginning to decrease.

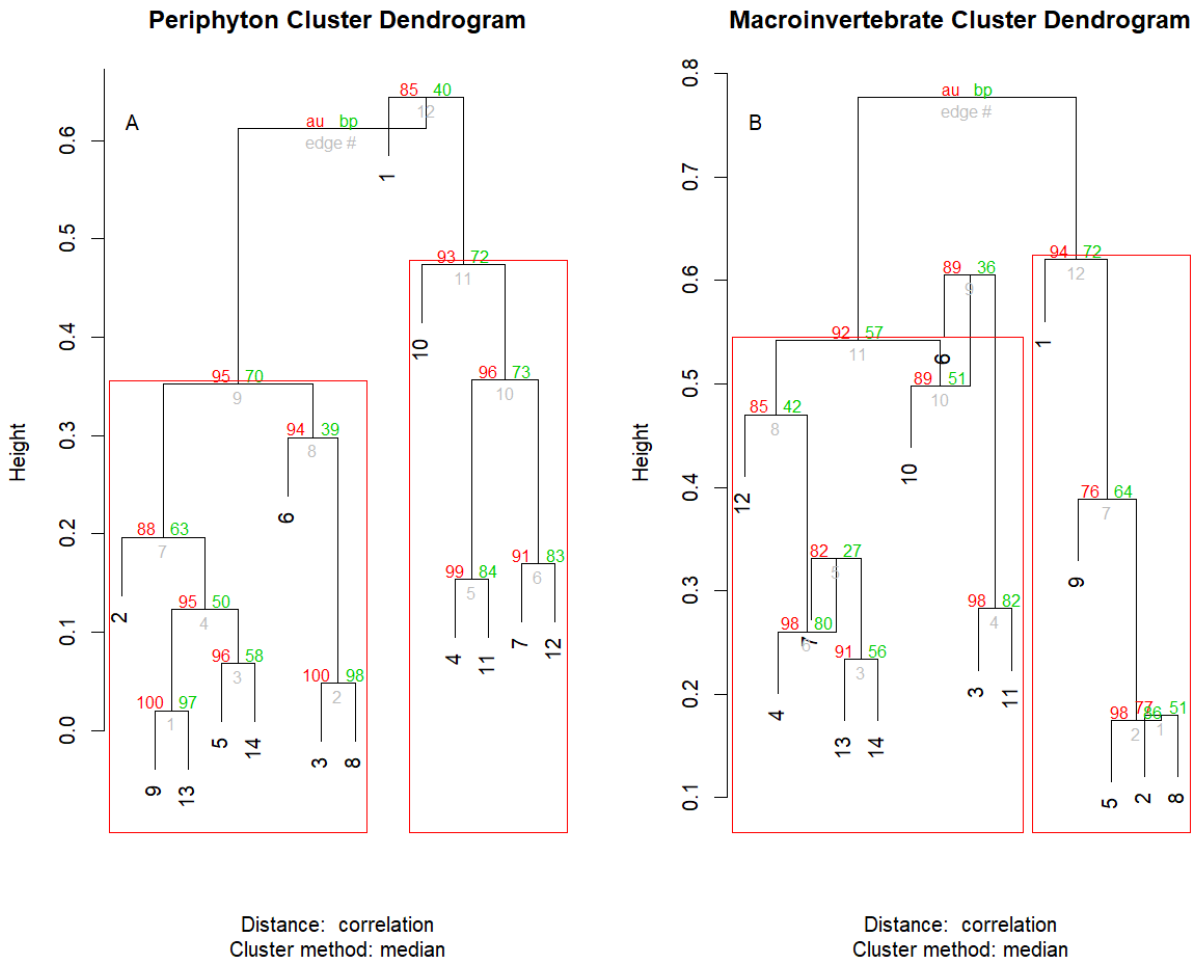

Figure S3: Weighted Pair-Group Centroid Clustering (WPGMC) for periphyton (A) and macroinvertebrate (B) community compositions. Approximately unbiased (au) p-values are computed by multiscale bootstrap resampling, and displayed in red on the left side of each node. Bootstrapped probabilities (BP) are displayed in green on the right side of each node. Unlike k-mediods, WPGMC uses a hierarchical approach to assign clusters, which are bootstrapped in order to generated a probability of group membership. This technique suggested that both periphyton and macroinvertebrates could be grouped in two clusters. Grouping macroinvertebrates into three clusters was possible; however, three clusters resulted in 8 of the 14 sampling locations being assigned to a group. In contrast, two groups enabled 13 of the 14 sampling locations to be assigned to a cluster.

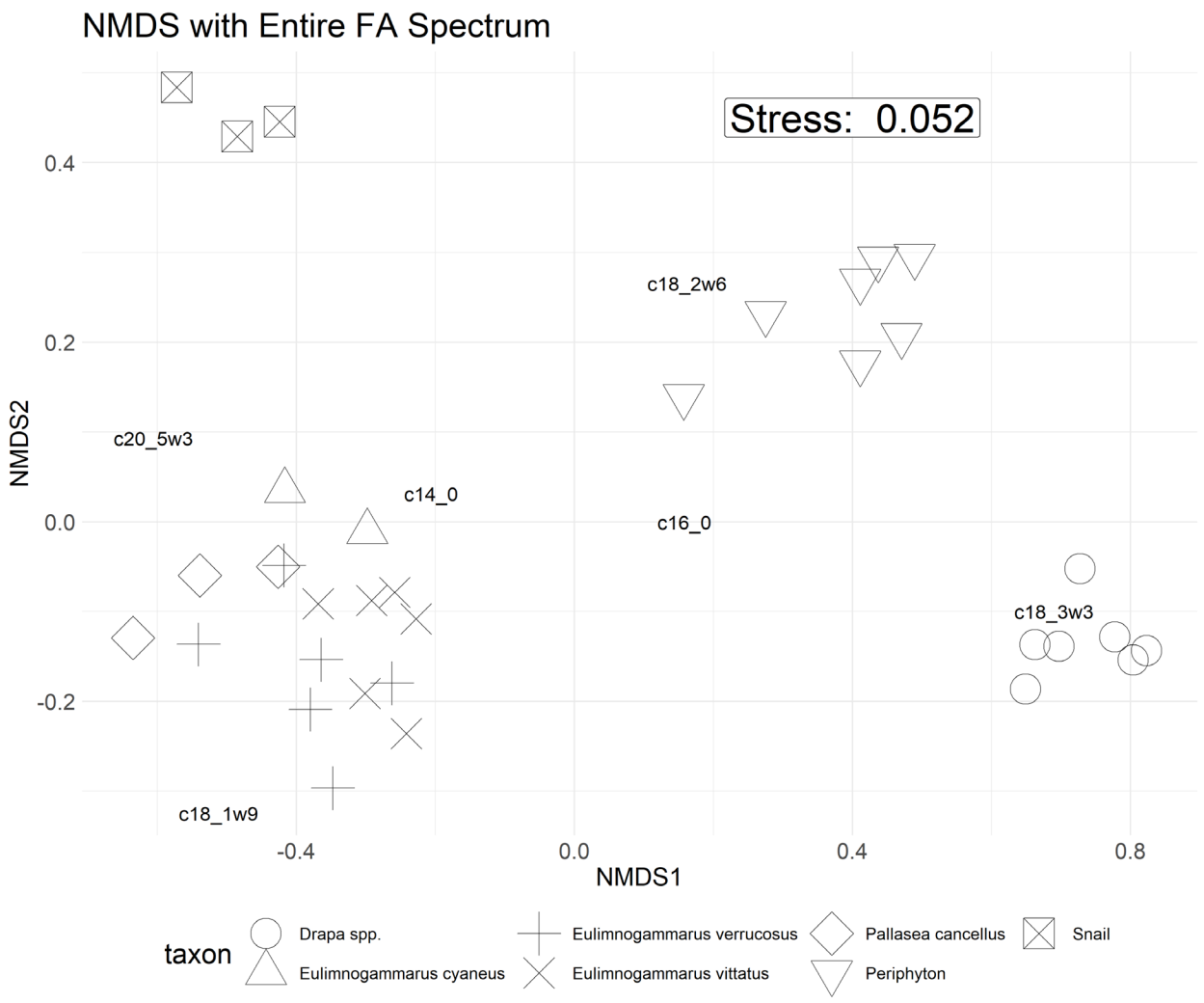

Figure S2: NMDS with Bray-Curtis dissimilarity of proportional fatty acid compositions for each macroinvertebrate and primary producer collected. *Eulimnogammarus* and *Pallasea* are endemic amphipod genera. *Drapa* are endemic filamentous algae that are large and form very dense mats easily collected where it occurs. *Drapa* occurred in large, visible colonies, allowing us to sample and analyze just the *Drapa* fatty acids. Because *Drapa* fatty acids were dominated by 18:3ω3 more so than periphyton, they formed their own cluster. Snails were not identified to species prior to fatty acid analysis. Interspecific variation in fatty acid composition tended to be larger than intraspecific variation, implying that fatty acid signatures were largely species-specific and not environmentally driven.

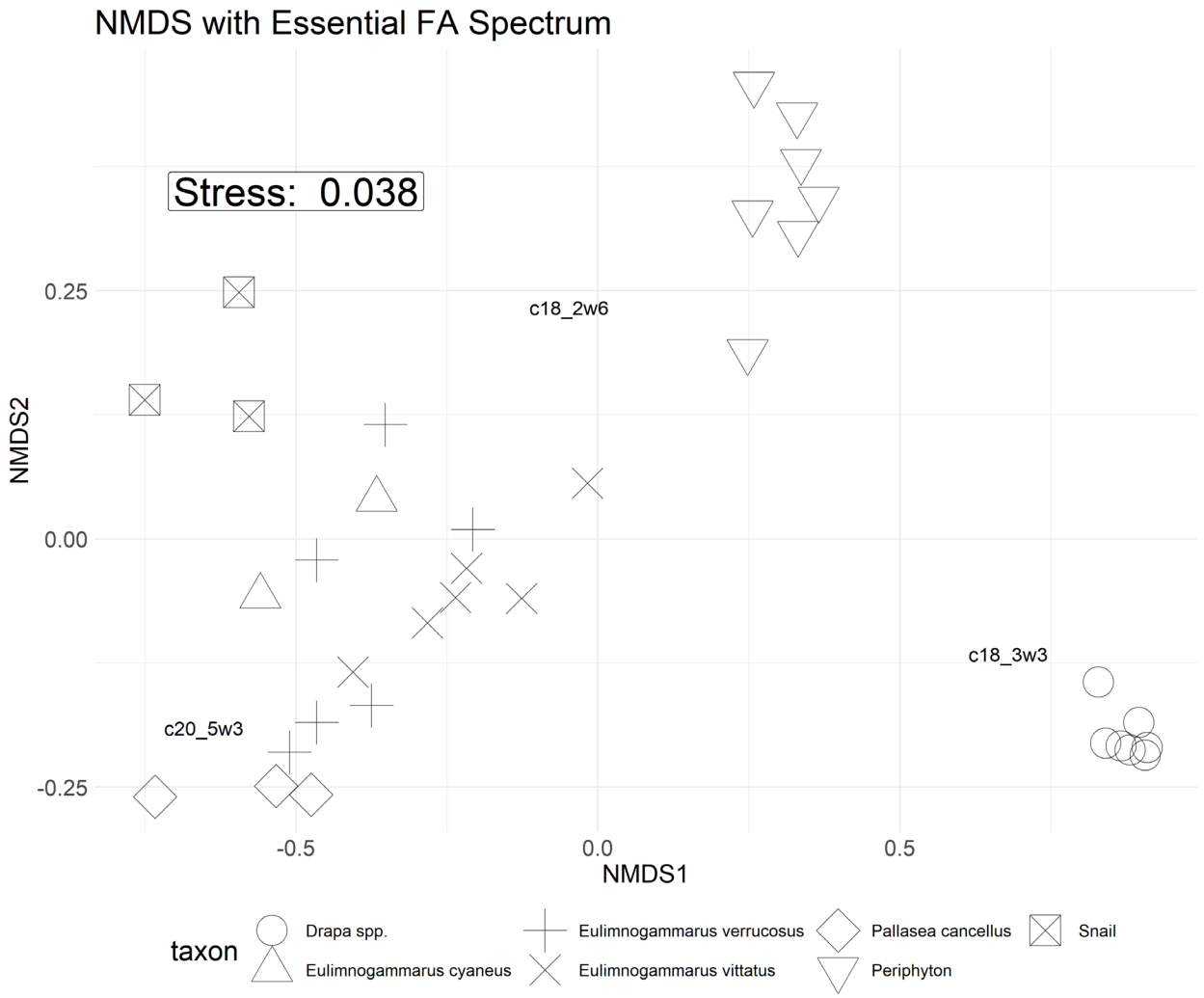

Figure S3: NMDS with Bray-Curtis dissimilarity of proportional biologically essential fatty acid compositions for each macroinvertebrate and primary producer collected. *Eulimnogammarus* and *Pallasea* are endemic amphipod genera. *Drapa* are endemic filamentous algae that are large and form very dense mats easily collected where it occurs. *Drapa* occurred in large, visible colonies, allowing us to sample and analyze just the *Drapa* fatty acids. Because *Drapa* fatty acids were dominated by 18:3ω3 more so than periphyton, they formed their own cluster. Snails were not identified to species prior to fatty acid analysis. Interspecific variation in fatty acid composition tended to be larger than intraspecific variation, implying that fatty acid signatures were largely species-specific and not environmentally driven.

Table S2: Fatty acid groupings used in this analysis	
Fatty Acid Group	Fatty acids considered
Branched	a-15:0, i-15:0, a-17:0, i-17:0
SAFA	12:0, 14:0, 15:0, 16:0, 17:0, 18:0, 20:0, 22:0, 24:0
MUFA	14:1n-5, 15:1ω7, 17:1n7, 16:1ω5, 16:1ω6, 16:1ω7, 16:1ω8, 16:1ω9, 18:1ω7, 18:1ω9, 20:1ω7, 20:1ω9, 22:1ω7, 22:1ω9
SCPUFA	16:2ω4, 16:2ω6, 16:2ω7, 16:3ω3, 16:3ω4, 16:3ω6, 16:4ω1, 16:4ω3, 18:2ω6, 18:2ω6t, 18:3ω3, 18:3ω6, 18:4ω3, 18:4ω4, 18:5ω3
LCPUFA	20:2-5-11, 20:2-5-13, 20:2ω6, 20:3ω3, 20:3ω6, 20:4ω3, 20:4ω6, 20:5ω3, 22:2ω6, 22:3ω3, 22:4ω3, 22:4ω6, 22:5ω3, 22:5ω6, 22:6ω3

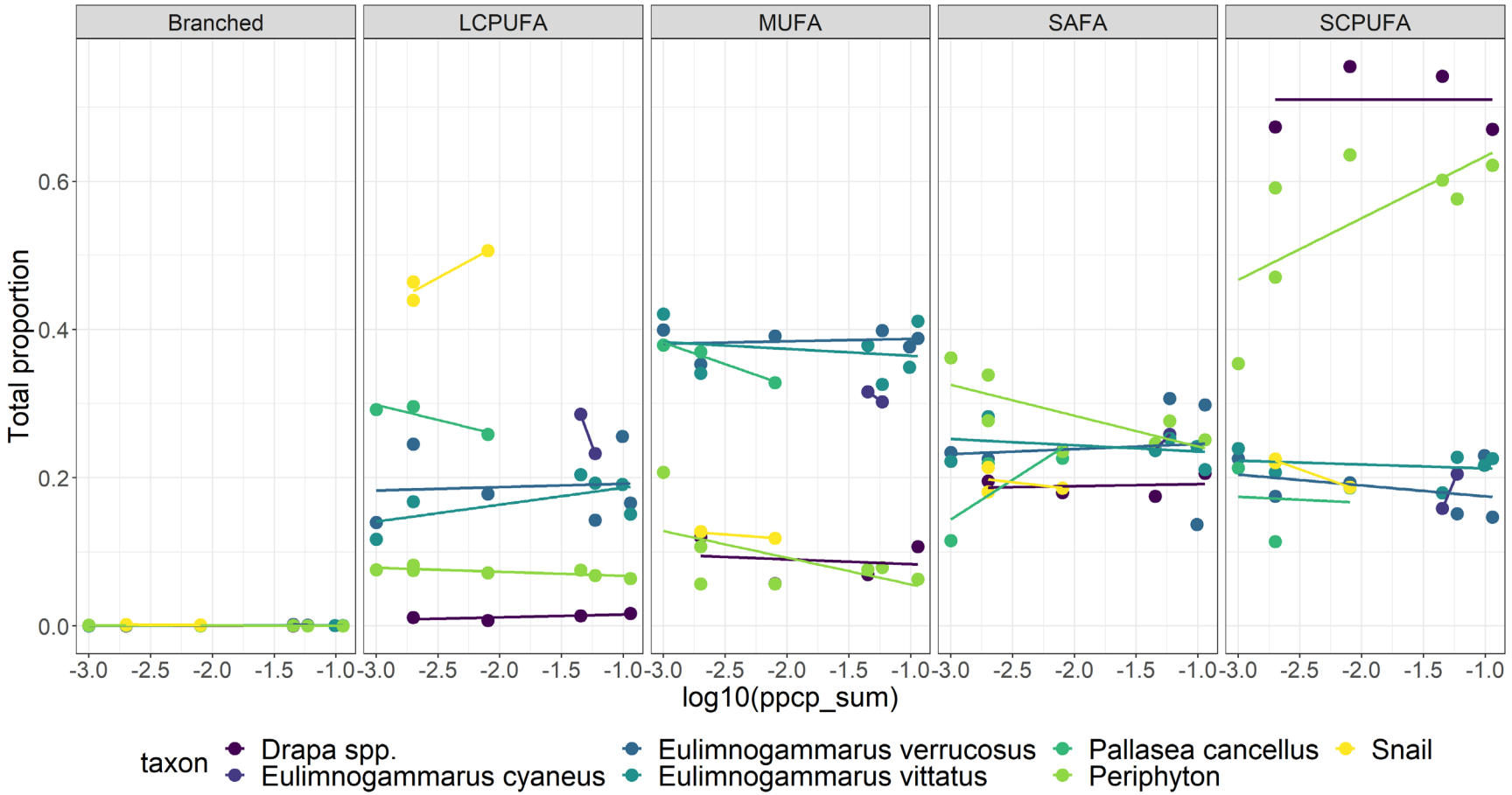

Figure S4: Proportions of major fatty aid groups (as defined in Table S2) across the sewage gradient. Primary producers (Drapa spp. and periphyton) were largely characterized by SCPUFAs, amphipods were largely associated with high MUFA abundance, and snails were generally characterized with high LCPUFA abundance. Across the sewage gradient, periphyton SCPUFA tended to increase, which lead to more targeted analyses on which specific fatty acids were increasing. In contrast periphyton, all other taxa remained consistent with respect to fatty acid proportions across the sewage gradient.

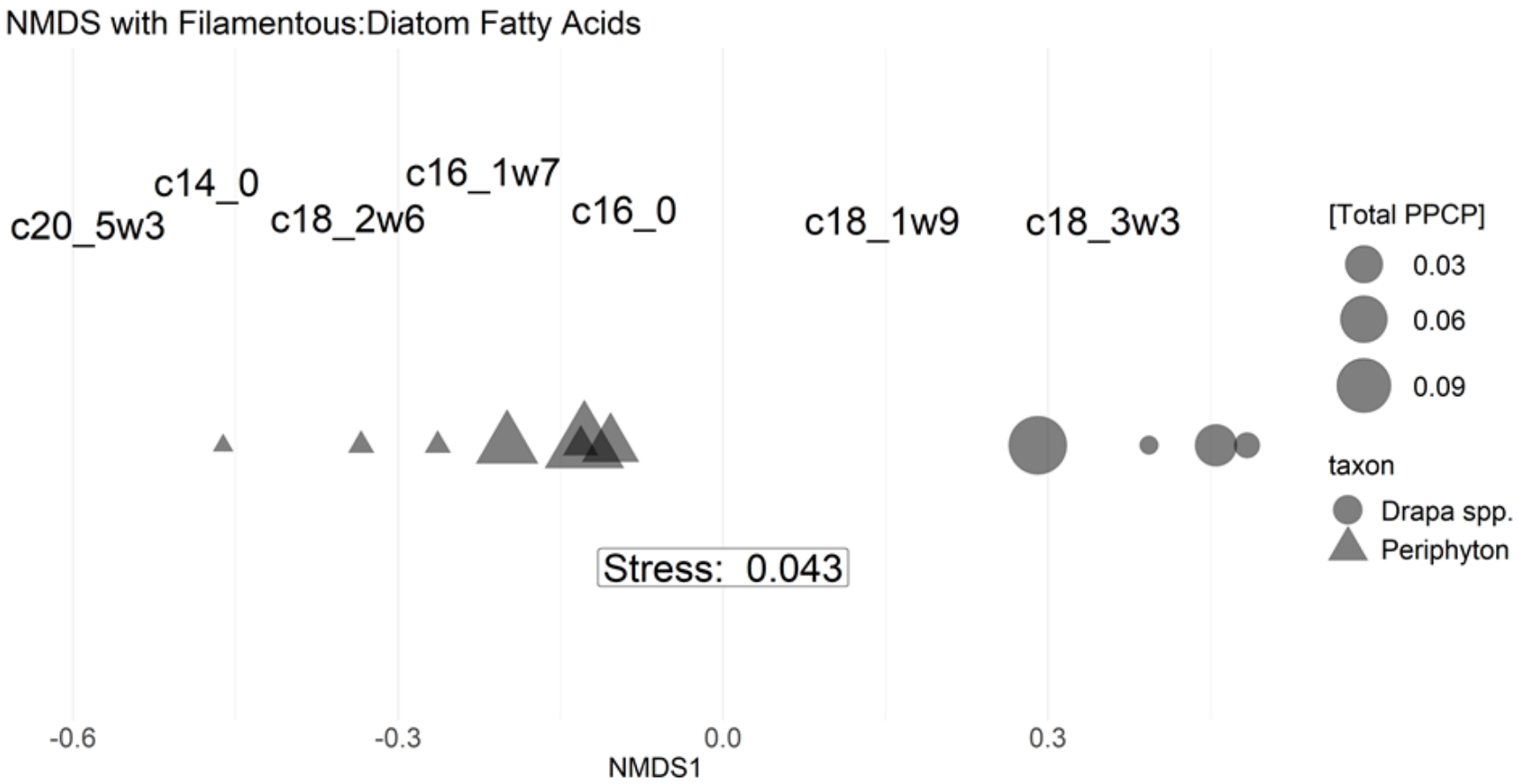

Figure S5: One-dimensional NMDS with Bray-Curtis similarity of seven targeted fatty acids of interest for primary producers. Fatty acid species sores are placed above shapes. Shapes are sized by total PPP concentration. Periphyton (triangles) tend to increase from left-to-right, suggesting that periphyton tend to include more 18:3ω3 and 18:1ω9 (indicators of green algal taxa) with an increasing sewage signal. In contrast, Drapa spp. (circles) fatty acids tend to remain consistent across the sewage gradient.

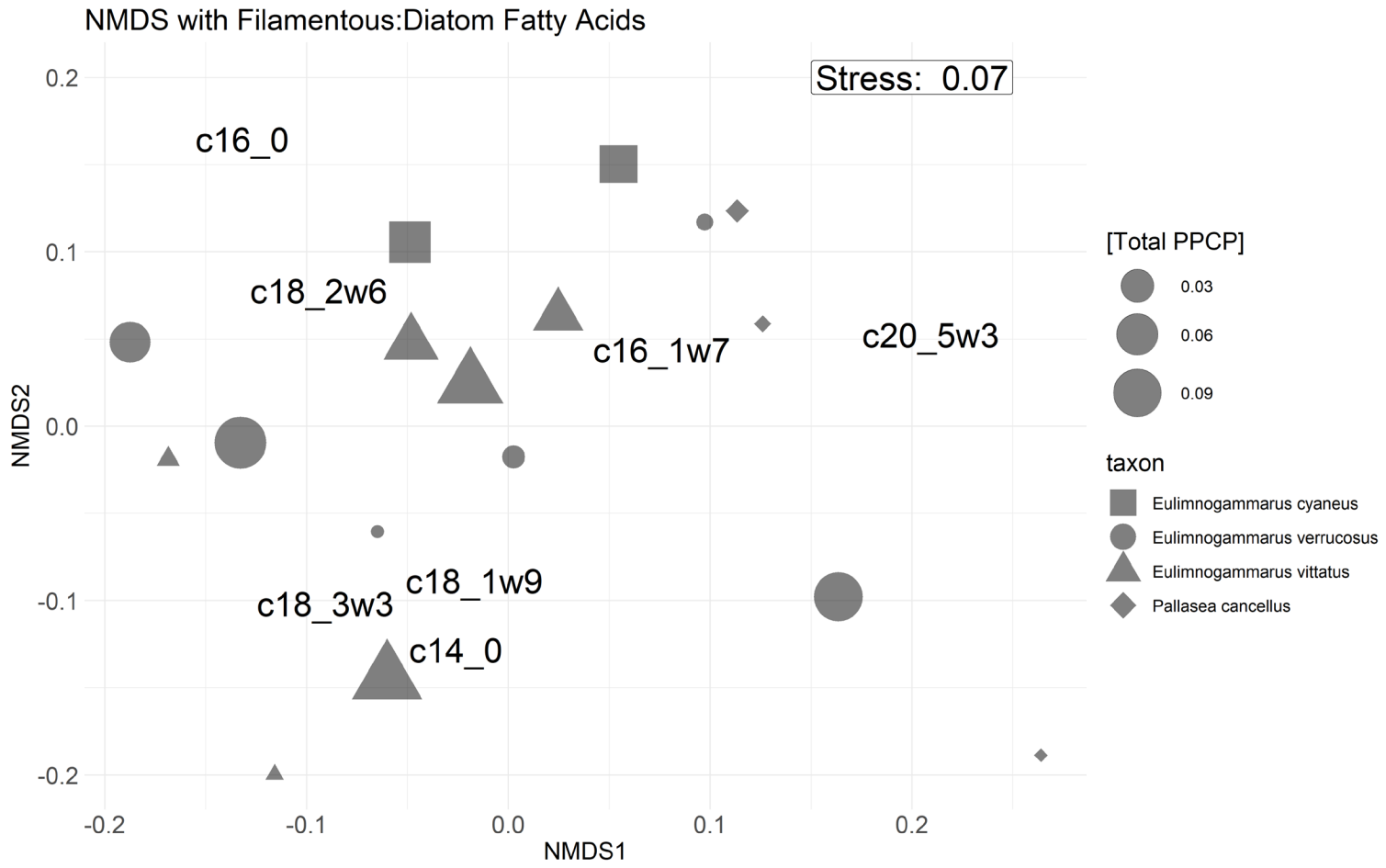

Figure S6: NMDS with Bray-Curtis similarity of seven targeted fatty acids of interest for primary producers. Fatty acid species sores are placed above shapes. Shapes are sized by total PPP concentration. Visually, there appears to be no distinct separation among or within taxa unlike was observed with periphyton (Figure S5).

1169